A Quantitative Investigation of Selected Reactions in the Fibrinolytic Cascade

by

P. Michael Cook

A thesis submitted to the Department of Biochemistry
in conformity with the requirements for
the degree of Master of Science

Queen's University
Kingston, Ontario, Canada
January, 2008

Abstract

Previous work has shown that thrombin activatable fibrinolysis inhibitor (TAFI) was unable to prolong lysis of purified clots in the presence of Lys-plasminogen (Lys-Pg), indicating a possible mechanism for fibrinolysis to circumvent prolongation mediated by activated TAFI (TAFIa). Therefore, the effects of TAFIa on Lys-Pg activation and Lys-plasmin (Lys-Pn) inhibition by antiplasmin (AP) were quantitatively investigated using a fluorescently labeled recombinant Pg mutant which does not produce active Pn. High molecular weight fibrin degradation products (HMW-FDPs), a soluble fibrin surrogate that models Pn modified fibrin, treated with TAFIa decreased the catalytic efficiency (k_{cat}/K_m) of 5IAF-Glu-Pg cleavage by 417-fold and of 5IAF-Lys-Pg cleavage by 55-fold. A previously devised intact clot system was used to measure the apparent second order rate constant (k_2) for Pn inhibition by AP over time. While TAFIa was able to abolish the protection associated with Pn modified fibrin in clots formed with Glu-Pg, it was not able to abolish the protection in clots formed with Lys-Pg. However, TAFIa was still able to prolong the lysis of clots formed with Lys-Pg.

TAFIa prolongs clot lysis by removing the positive feedback loop for Pn generation. The effect of TAFIa modification of the HMW-FDPs on the rate of tissue type plasminogen activator (tPA) inhibition by plasminogen activator inhibitor type 1 (PAI-1) was investigated using a previously devised end point assay. HMW-FDPs decreased the k_2 for tPA inhibition rate by 3-fold. Thus, HMW-FDPs protect tPA from PAI-1. TAFIa treatment of the HMW-FDPs resulted in no change in protection. Vitronectin also did not appreciably affect tPA inhibition by PAI-1. Pg, in conjunction with HMW-FDPs, decreased the k_2 for tPA inhibition by 30-fold. Hence, Pg, when bound to HMW-FDPs,

protects tPA by an additional 10-fold. TAFIa treatment of the HMW-FDPs completely removed this additional protection provided by Pg. In conclusion, an additional mechanism was identified whereby TAFIa can prolong clot lysis by increasing the rate of tPA inhibition by PAI-1 by eliminating the protective effects of Pn-modified fibrin and Pg. Because TAFIa can suppress Lys-Pg activation but cannot attenuate Lys-Pn inhibition by AP, the Glu- to Lys-Pg/Pn conversion is able to act as a fibrinolytic switch to ultimately lyse the clot.

Acknowledgements

There are many individuals who deserve recognition for their role in the completion of this thesis. Foremost is my supervisor, Dr. Michael Nesheim, whose skill as a scientist, passion for rigorous quantitative investigation, and talent as an educator have shaped and guided me throughout the research process. I also thank Tom Abbott for his cheerful assistance in navigating the systems (and reams of paperwork) that underlie all aspects of this research. I am grateful to my parents, Blake and Arlene, and Nona for their unwavering love and support as I pursue my goals. Finally, I thank my wife, Jennifer, for listening to me talk about my work with empathy, laughter, and patience.

Table of Contents

List of Tables

List of Figures

List of Abbreviations

AP	α_2-antiplasmin
DSPAα1	*Desmodus rotundus* salivary plasminogen activator α1
FDPs	fibrin degradation products
HBS	HEPES buffered saline (20 mM HEPES, 150 mM NaCl, pH 7.4)
HBST	20 mM HEPES, 150 mM NaCl, 0.01% Tween 80, pH 7.4
HMW-FDPs	high molecular weight FDPs
k_2	apparent second order rate constant for inhibition
k_{cat}	catalytic rate constant
K_m	Michaelis constant
k_{cat}/K_m	catalytic efficiency
K_d	dissociation constant
K_S	K_m for the enzyme catalyzed hydrolysis of a chromogenic substrate
K_P	K_d for Pg binding to HMW-FDPs
K_A	K_d for tPA binding to HMW-FDPs
K_{PA}	binding constant for tPA binding to the HMW-FDP:Pg complex
K_{AP}	binding constant for Pg binding to HMW-FDP:activator complex
PAI-1	Pg activator inhibitor type 1
PC	protein C
aPC	activated protein C
Pg	plasminogen
Glu-Pg	Pg variant that has Glu1 as the first residue
Lys-Pg	Pg variant that has Lys78 as the first residue
5IAF-Pg	5-iodoacetamidofluorescein labeled Pg mutant (S741C)
Pn	plasmin
Glu-Pn	Pn variant that has Glu1 as the first residue
Lys-Pn	Pn variant that has Lys78 as the first residue
PPAck	Phe-Pro-Arg chloromethylketone
TAFI	thrombin activatable fibrinolysis inhibitor
TAFIa	activated TAFI
tPA	tissue type plasminogen activator
sc-tPA	single chain tPA
tc-tPA	two chain tPA
Vn	vitronectin

1. Introduction

Extensive regulation is required to properly balance the coagulation and fibrinolytic cascades: if tilted towards coagulation , the body is at risk of developing pathological thrombi, leading to myocardial infarctions and ischemic strokes; if tilted towards fibrinolysis, the body is at risk of hemorrhage (Fig. 1-1). In response to a vascular injury, thrombin, the terminal enzyme in the coagulation cascade, cleaves fibrinogen (Fg), which spontaneously polymerizes to form a fibrin clot. Once formed, fibrin serves as a template for plasminogen (Pg) activation to plasmin (Pn) by tissue type Pg activator (tPA). Pn ultimately degrades the insoluble fibrin clot into soluble fibrin degradation products (FDPs).

Fg, one of many thrombin targets, is a symmetrical dimer made up of two Aα chains, two Bβ chains, and two γ chains (1). Its overall shape resembles a dumbbell (2): a central globular E domain, containing the amino termini of the chains, is connected to two D domains, containing the carboxyl termini, by coiled coil helices (3-6). Thrombin cleaves fibrinopeptide A, causing Fg monomers to spontaneously polymerize to form double stranded protofibrils (7). In polymerized fibrin, D domains in adjacent Fg monomers non-covalently interact with the E domain of a third monomer on the opposing strand (Fig. 1-2). Fibrinopeptide B cleavage causes the protofibrils to associate forming the fibrin network (7). Fibrin is further strengthened by the transglutaminase factor XIIIa which creates an isopeptide bond between two γ chains in neighbouring D domains (8-10). Only a small amount of thrombin (~25 nM) generated by the extrinsic pathway is required to form the fibrin clot (11). Almost immediately after clotting, a large, transient burst of thrombin (~850 nM) accumulates due to a positive feedback loop caused by

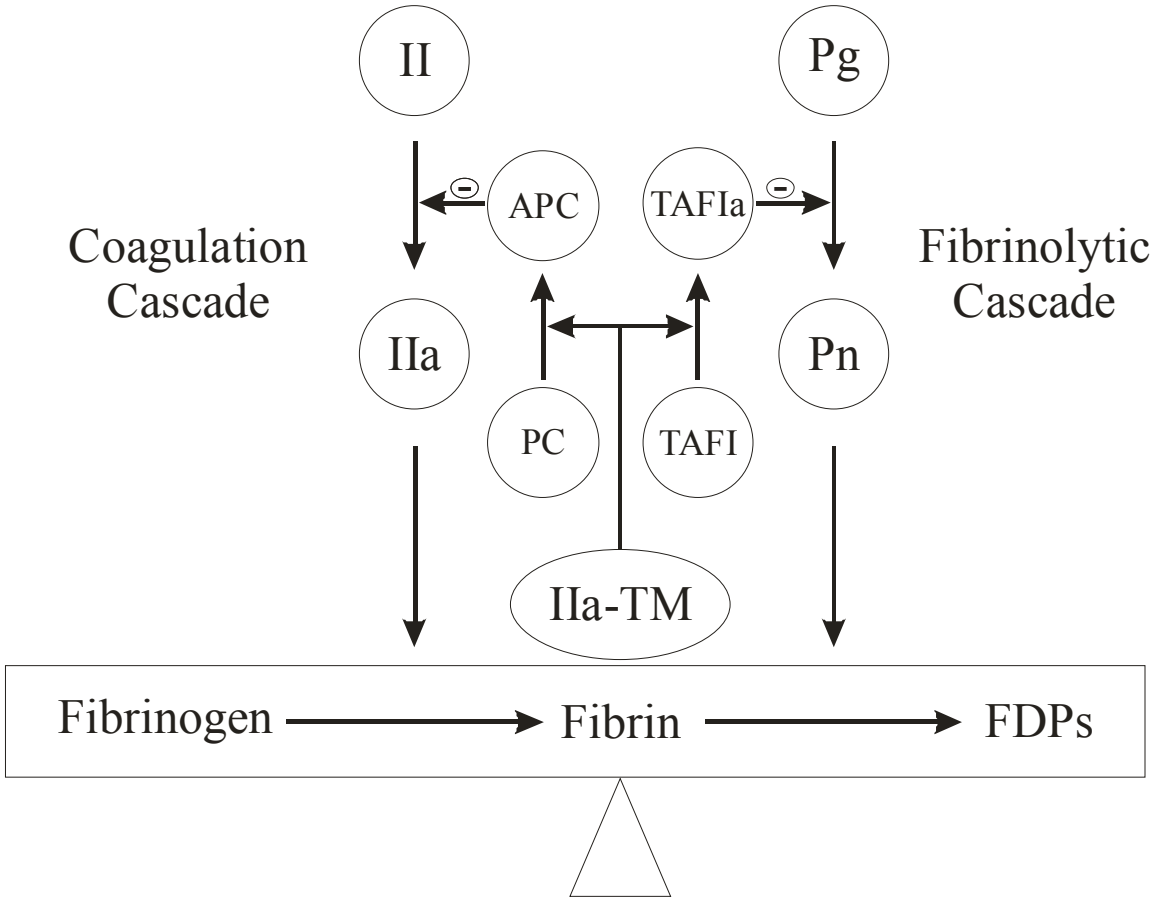

Figure 1-1. The balance between coagulation and fibrinolysis. (Adapted from M. Nesheim (11)) Upon injury, the coagulation cascade forms thrombin (IIa) from prothrombin (II). Thrombin cleaves fibrinopeptides A and B from soluble fibrinogen, which spontaneously polymerizes forming an insoluble fibrin clot at the site of injury. Fibrin serves as a cofactor for Pg activation to Pn. Pn degrades the fibrin clot into soluble fibrin degradation products (FDPs). Thrombin can also bind thrombomodulin (TM) in order to activate PC and TAFI. aPC attenuates coagulation by inactivating factors Va and VIIIa, whereas TAFIa attenuates fibrinolysis by decreasing the cofactor activity of fibrin for Pg activation.

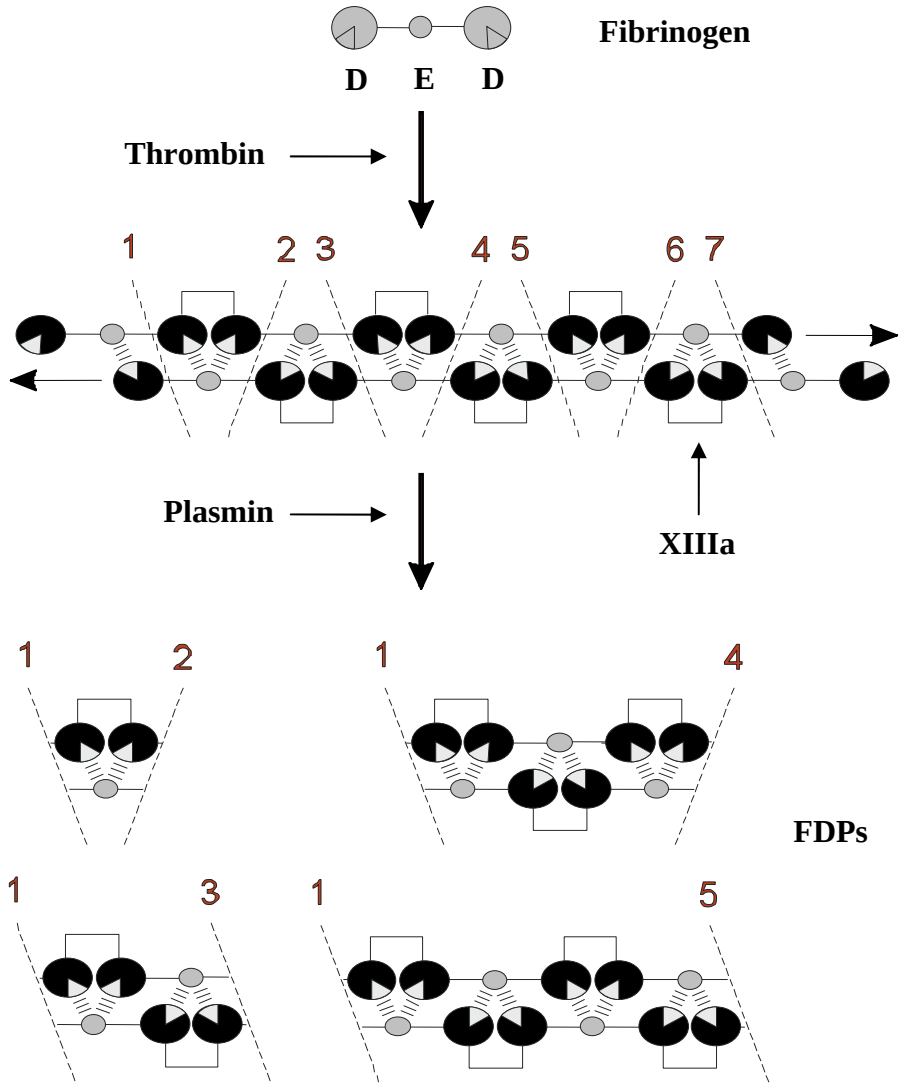

Figure 1-2. Fibrin formation and degradation. (Adapted from Walker and Nesheim (12)) Fg is a soluble monomer consisting of two Aα, two Bβ, and two γ chains. A central E domain is connected by coiled coil helices to two D domains. Thrombin cleavage of fibrinopeptides A and B on Fg results in its spontaneous polymerization. Adjacent D domains non-covalently interact with the E domain on the opposing strand of the protofibril. Factor XIIIa stabilizes fibrin by catalyzing the formation of an isopeptide bond between adjacent γ chains. Once formed, Pn cleaves each of the α, β, and γ chains to release soluble FDPs, thereby lysing the clot. Depending on the cleavage site, FDPs of various sizes are released. The smallest FDP is approximately 260 kDa and consists of two D domains and an E domain. The largest FDP observed experimentally is approximately 10 million Da which would contain approximately 40 intact fibrin monomers.

thrombin mediated cleavage of factors V and VIII. The role of this feedback mechanism is to stabilize the clot by activating factor XIII and to localize the clot to the site of injury by activating protein C (PC).

After the fibrin network has been sufficiently constructed at the site of injury, further clotting ceases, avoiding unnecessary blockage to the blood vessel. When the growing fibrin clot reaches the endothelium, thrombin binds to the membrane protein thrombomodulin. This protein switches the activity of thrombin from a procoagulant to an anticoagulant and an antifibrinolytic (13-15). Thrombomodulin contains an intracellular domain, a transmembrane domain, a Ser/Thr rich domain, six EGF domains, and a lectin like domain (15,16). EGF domains 4-6 plus the linker region between EGF domains 3 and 4 are required for thrombin-thrombomodulin to activate PC to its activated form (aPC) (17,18). aPC inactivates coagulation factors Va and VIIIa by proteolytic cleavage (19-21).

Once formed, fibrin serves as a cofactor in its own degradation by acting as a scaffold or template for Pg activation to Pn by tPA (Fig. 1-3). Pg consists of five kringle domains and a protease domain (22). Each kringle contains a lysine binding site, which collectively mediate binding to fibrin. Kringles 1 to 4 bind lysine, to which kringle 5 has no affinity, but kringles 1, 4, and 5 bind εACA, a carboxyl terminal lysine analog, to which kringle 2 has a weak affinity and kringle 3 does not bind (22-30). tPA is the main physiological Pg activator in terms of fibrinolysis because the reaction is critically dependent on fibrin as a cofactor. In the absence of fibrin, Pg activation by tPA occurs very slowly; in the presence of fibrin, Glu- and Lys-Pg activation are enhanced 413- and 1881-fold (31). tPA consists of a finger domain, an epidermal growth factor like domain,

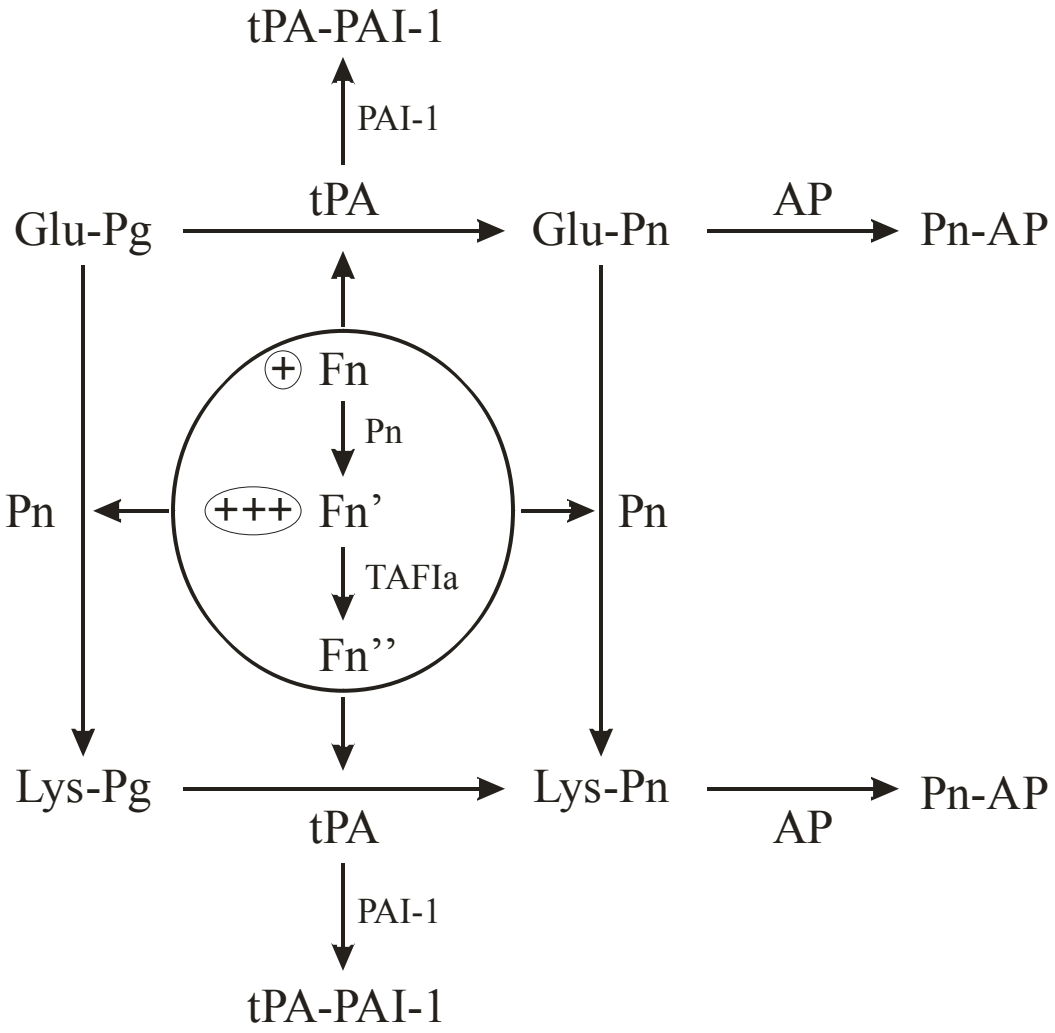

Figure 1-3. An overview of Pg activation and its regulation. Fibrin acts as a cofactor for its own degradation. Once formed, intact fibrin (Fn) supports Pg activation to Pn by tPA. Before lysing the clot, Pn cleavage at individual Fn chains generates carboxyl-terminal lysine and arginine residues. The result is Pn modified fibrin (Fn'), which has a 3-fold greater cofactor activity than Fn. TAFIa, a carboxypeptidase, can remove these residues, generating TAFIa modified fibrin (Fn''). This form of fibrin has a decreased cofactor activity. Pn also removes the N-terminal 77 amino acids from Glu-Pg, generating Lys-Pg, a better substrate for tPA mediated activation. TAFIa removes the positive feedback loop associated with Pn modification of fibrin and Glu-Pg. Fibrinolysis is also down regulated by the inhibitors PAI-1 and AP, which inhibit tPA and Pn respectively.

two kringle domains, and a protease domain (32). tPA binds fibrin in a lysine dependent manner through its kringle 2 domain and in a lysine independent manner via its finger domain (33). Finger dependent binding appears to be the primary interaction between tPA and fibrin. tPA mutants lacking the finger domain displayed decreased fibrin binding and Pg activation, whereas these properties were unaffected in tPA mutants lacking the kringle 2 domain (31). tPA, secreted by endothelial cells as a single chain polypeptide (34), can be cleaved by Pn at Arg275 forming two chain tPA (tc-tPA). This cleavage is not the typical zymogen to enzyme conversion seen in the coagulation and fibrinolytic cascades. Single chain tPA (sc-tPA) and tc-tPA have virtually identical fibrinolytic properties, namely Pg activation and lysis (35). The only difference between the two is that tc-tPA is inhibited faster than sc-tPA by its physiological inhibitor plasminogen activator inhibitor type 1 (PAI-1) (36-38).

Before completely digesting the fibrin clot, Pn modifies the fibrin surface, exposing carboxyl-terminal lysine and arginine residues. tPA and Pg bind the lysine residues, resulting in an up regulation of Pg activation by tPA; Pn modified fibrin has a 3-fold higher cofactor activity for Pg activation than intact fibrin (39). In addition to modifying fibrin, Pn also proteolytically removes the 77 amino terminal residues from Glu-Pg to form the truncated Lys-Pg (40,41). Lys-Pg is a roughly 20 fold better substrate on fibrin than Glu-Pg (31). In essence, Pn action on fibrin and Glu-Pg results in a positive feedback loop for Pn generation to quickly remove the fibrin clot. To prevent rapid lysis immediately after clotting, mechanisms exist to maintain the fibrin clot while the injury is repaired.

Thrombin activatable fibrinolysis inhibitor (TAFI, also known as

procarboxypeptidase U (42), plasma procarboxypeptidase B (43), and carboxypeptidase R (44)), depicted in Fig. 1-4A, is a 60 kDa plasma glycoprotein that circulates at approximately 75 nM. Thrombin-thrombomodulin activates TAFI by proteolytic cleavage at the Arg92-Ala93 peptide bond (45). The activation peptide (residues 1-92) is released upon activation, generating activated TAFI (TAFIa) (residues 93-401). The activation mechanism is described by an enzyme central model (Fig. 1-4B). According to this mechanism, thrombin can interact with either TAFI or thrombomodulin to produce the corresponding binary complexes. These complexes can interact with the third component to form the ternary thrombin-thrombomodulin-TAFI complex from which TAFIa is generated.

TAFIa, a carboxypeptidase, removes the carboxyl terminal lysine and arginine residues exposed by Pn on fibrin, thereby attenuating fibrinolysis (46). This TAFIa modified fibrin compared to Pn modified fibrin is approximately 90-fold less effective as a cofactor for tPA mediated Glu-Pg activation (39) and has a decreased ability (12-fold) to protect Pn from α_2-antiplasmin (AP) inhibition (47). The net result of TAFIa modification of fibrin is to eliminate the positive feedback mechanism for Pg activation and to suppress Pn levels within the fibrin clot (Fig. 1-3).

An additional 13 residues on EGF 3 in thrombomodulin not needed for PC activation are required for TAFI activation by thrombin-thrombomodulin (18). Thrombomodulin binds to exosite 1 on thrombin via EGF 5 (48). It does not alter the active site of thrombin as one theory postulated (49,50), but effectively blocks any procoagulant substrates from binding. The crystal structure of thrombin bound to a construct of thrombomodulin truncated from the amino terminus showed no alteration in the thrombin

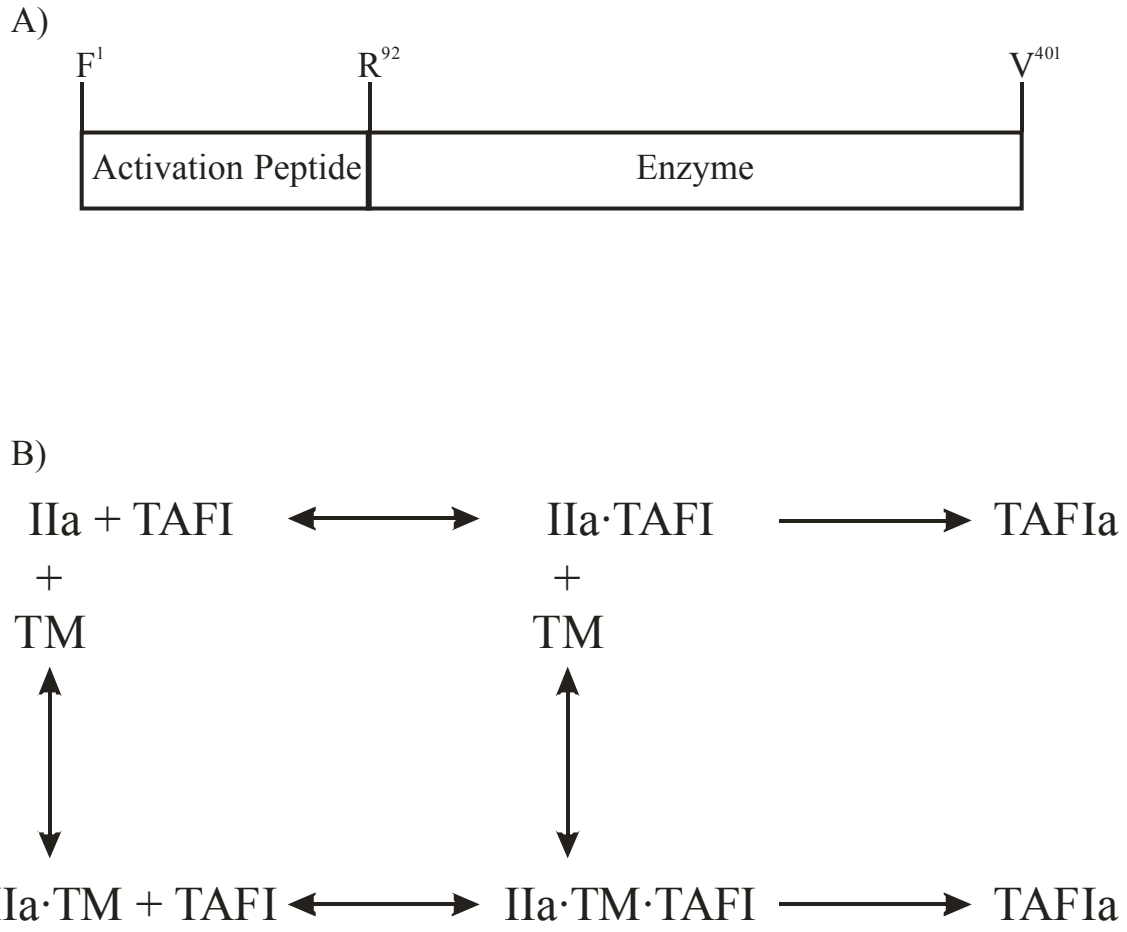

Figure 1-4. The enzyme central model of TAFI activation. (Adapted from Bajzar *et al.* (45)) Thrombin (IIa) can interact with TAFI or thrombomodulin (TM), forming one of two possible binary complexes. TM or TAFI can then interact with these complexes to form a ternary IIa·TM·TAFI complex. IIa, in the ternary or the IIa·TAFI binary complex, cleaves TAFI at Arg92, removing the activation peptide and forming the carboxypeptidase TAFIa.

active site (48). Furthermore, replacing the thrombin cleavage site in TAFI with the corresponding site from fibrinogen did not alter the thrombomodulin dependence of TAFI activation (51).

Thrombin-thrombomodulin is the primary TAFI activator *in vivo*, but thrombin and plasmin have also been shown to activate TAFI (52,53). Thrombin-thrombomodulin accelerates TAFI activation by 1250-fold over thrombin alone (45) and 150-fold over Pn (53). Through thrombin and Pn catalyze TAFI activation at a much slower rate than thrombin-thrombomodulin, these reactions remain relevant. Others have shown that TAFI activation occurs after clotting and again during lysis (54). Even in the absence of thrombomodulin, considerable TAFIa is generated over the course of clotting and lysis (unpublished observations by J.H. Foley and M.E. Nesheim). However, the role of TAFIa generated during lysis, presumably by Pn, is at present unclear and under investigation.

TAFIa has no known inhibitors in plasma; its inactivation is regulated by its thermal instability. Two single nucleotide polymorphisms that result in an altered amino acid sequence have been identified in TAFI (55-57). The polymorphism at position 147 (Ala/Thr) has no effect on thermal stability (57). The TAFI variant with an Ile at amino acid 325 has a half-life of 15 min at 37°C, whereas the Thr variant has an eight minute half-life (57). Reversible TAFIa inhibitors can extend these half-lives by stabilizing the enzyme (58). In fact, at low concentrations, these inhibitors actually increase the antifibrinolytic potential of TAFIa (59,60).

No doubt, TAFIa is essential for clot stability and suppression of lysis. One hypothesis regarding hemophilia is that these patients can adequately form clots but lack

the thrombin burst, and therefore TAFI activation, to effectively stabilize the clot. As a result, hemophiliacs lyse their clots prematurely and cannot stop excessive blood loss. Previous work using hemophilic dogs showed that these animals were able to form, but not sustain, a clot (61). The hemophilic dogs had similar bleeding times as the normal dogs but would begin bleeding again shortly after and could not stop this secondary bleeding (61). Furthermore, the *in vitro* clot lysis times of hemophilic plasmas can be rescued by adding exogenous soluble thrombomodulin or by increasing the TAFI concentration (62,63).

Direction of the Current Studies. The current studies in fibrinolysis are directed at investigating an additional mechanism by which TAFIa is able to attenuate lysis and a potential mechanism whereby fibrinolysis can bypass TAFIa. TAFI and TAFIa have been shown to prolong lysis in both plasma and purified systems (52,64). However, TAFI did not prolong the lysis of clots formed from purified components with Lys-Pg, suggesting a hypothesis that fibrinolysis can escape TAFIa mediated prolongation (52). Because fibrin is insoluble, high molecular weight FDPs (HMW-FDPs) were used as a surrogate for Pn modified fibrin. These soluble degradation products support tPA mediated Glu-Pg activation much like intact fibrin. Furthermore, they contain carboxyl-terminal lysine and arginine residues which can be removed by TAFIa, generating a surface similar to TAFIa modified fibrin. While tPA mediated Glu-Pg activation kinetics on intact, Pn modified, and TAFIa modified fibrin have been quantitatively studied (31,39), similar experiments with Lys-Pg have only been performed on intact fibrin (31). As a result, a quantitative analysis was performed on Lys-Pg activation kinetics on untreated and TAFIa treated HMW-FDPs. While TAFIa modification of the HMW-

FDPs resulted in a reduced cofactor activity, the reduction was much less drastic than the decrease seen with Glu-Pg; the cofactor activity of TAFIa modified HMW-FDPs for Lys-Pg activation is similar to intact fibrin.

Previous work showed that TAFIa could abrogate the protection of Pn from AP inhibition offered by Pn modified fibrin (47). The role of TAFIa in the protection of Lys-Pn has not been quantified. Therefore, Lys-Pn inhibition by AP was quantitatively studied within an intact fibrin clot in real time. TAFIa, while prolonging lysis in the presence of Lys-Pg, did not appreciably affect the apparent second order rate constant (k_2) for Lys-Pn inhibition by AP. In other words, TAFIa was not able to attenuate the protection of Lys-Pn, in contrast to the observations on Glu-Pn protection.

A recent study showed that TAFIa markedly lowered the ability of HMW-FDPs to protect Pn from AP (65). Since tPA also binds to the fibrin surface via lysine residues (33,66-68), a similar protective phenomenon was hypothesized to occur with tPA and PAI-1. The protective effect of HMW-FDPs on tPA inhibition by PAI-1 was investigated, as well as to what extent TAFIa alters this effect. A previously described end point assay (65,69) was used to measure the k_2 for tPA inhibition by PAI-1. Similar to previous results, HMW-FDPs attenuate tPA inhibition by PAI-1. However, TAFIa treatment of the HMW-FDPs did not alter protection, contrary to the results seen with Pn inhibition by AP. End point assays performed using 5IAF-Pg resulted in further attenuation of tPA inhibition. TAFIa treatment of the HMW-FDPs eliminated the additional protection provided by 5IAF-Pg. An additional mechanism was indentified showing that TAFIa attenuates fibrinolysis by increasing the rate of tPA inhibition by PAI-1.

2. Experimental Procedures

Materials – Baby hamster kidney cells and the pNUT expression vector were a kind gift from Dr. Ross MacGillivray (University of British Columbia, Vancouver, British Columbia, Canada). The TAFI isoform with threonine residues at amino acid positions 147 and 325 was purified as previously described (70). Recombinant Pg(S741C), as described by Horrevoets *et al.* (71), was labeled with 5-iodoacetamidofluorescein to produce the catalytically inactive Pg derivative, 5IAF-Pg. Recombinant human tPA (Activase) was purchased from the hospital pharmacy at Kingston General Hospital (Kingston, Ontario, Canada). tc-tPA was made as previously described (46). Human thrombin was prepared from plasma derived prothrombin as previously described (12,72). The soluble thrombomodulin derivative Solulin was a kind gift from Dr. Oliver Kops (Paion, GmbH, Berlin, Germany). *Desmodus rotundus* salivary plasminogen activator α1 (DSPAα1) was a kind gift from Dr. Peter Bringmann (Schering, AG, Berlin, Germany). Hirudin, D-Val-Phe-Lys chloromethylketone, D-Phe-Pro-Arg chloromethylketone (PPAck), and PAI-1 were purchased from Calbiochem.

Human Fg Purification – Human Fg was purified from fresh, frozen, citrated plasma as previously described (12) with one modification. A 1.2% (final concentration) polyethylene glycol 8000 cut following the second 2M β-alanine precipitation was used instead of a 2% cut. Purified Fg was dialyzed into HBS (20 mM HEPES, 150 mM NaCl, pH 7.4), aliquoted, snap frozen in liquid nitrogen, and stored at -80°C.

HMW-FDP Isolation – HMW-FDPs were purified from the lysis of a purified fibrin clot similar to methods described previously (73). A 6 mL fibrin clot was formed by adding 5 nM thrombin to 7.5 mg/mL Fg, 2 mM $CaCl_2$, and 40 nM Pn in HBS. Clotting

and subsequent lysis were monitored by absorbance at 800 nm in Lambda 25 spectrophotometer (PerkinElmer Life Sciences, Montreal, Quebec, Canada). When the signal decreased to 75% of its maximum, the reaction was stopped by addition of 5 μM PPAck and 5 μM D-Val-Phe-Lys chloromethylketone to inhibit the thrombin and Pn respectively. After vortexing briefly, the NaCl concentration was increased to 0.5 M by addition of solid NaCl. The mixture was then centrifuged at 5000 g for 10 min at 4°C. The supernatant was passed over a 30 mL Sephacryl S-1000 gel filtration column at 4°C by fast protein liquid chromatography in 20 mM HEPES, 0.5 M NaCl, pH 7.4 at 0.3 mL/min. Protein containing fractions were identified by absorbance at 280 and 320 nm. Each 1 mL fraction was assayed for its ability to stimulate DSPAα1 mediated 5IAF-Pg cleavage. 50 μg/μL of each fraction was incubated with 200 nM 5IAF-Pg in HBS, and the reaction was started with 20 nM DSPAα1 (100 μL total volume). The opaque 96-well Microfluor plate was blocked overnight with HBS, 1% Tween 80 before use to minimize non-specific binding to the plastic. The reaction was monitored by fluorescence in a Spectramax Gemini XS fluorescence plate reader (Molecular Devices, Sunnyvale, CA) using a 490 nm excitation wavelength, a 535 nm emission wavelength, and a 530 nm emission cutoff filter. Fractions that had a specific activity (initial rate divided by absorbance at 280 nm corrected for scatter) greater than 0.01 s^{-1} were pooled. Aliquots were snap frozen in liquid nitrogen and stored at -80°C.

TAFIa Treated HMW-FDP Production – TAFI (1 μM final concentration) was activated with 25 nM thrombin, 100 nM Solulin, 2 mM $CaCl_2$ in HBS, 0.01% Tween 80 (HBST) for 20 min at 25ºC. The thrombin was then inhibited with 200 nM (final concentration) hirudin. The mixture was placed on ice to minimize spontaneous thermal

inactivation.

The HMW-FDPs were then treated with TAFIa to remove the carboxyl-terminal lysine and arginine residues. TAFIa (10 nM final concentration) was incubated with 1 μM (final concentration) HMW-FDPs for 20 min at 25ºC. Following incubation, the TAFIa was inhibited with 200 nM potato tuber carboxypeptidase inhibitor (PTCI). Again, aliquots were snap frozen in liquid nitrogen and stored at -80°C.

5IAF-Pg Binding to HMW-FDPs – To quantify the affinity of 5IAF-Pg for HMW-FDPs, the change in fluorescein fluorescence upon binding was monitored in an LS50B Luminescence Spectrometer (Perkin Elmer Life Sciences). Fluorescein was excited at 490 nm with a 2.5 nm slit width and emission was detected at 535 nm with a 10 nm slit width and a 510 nm emission cutoff filter. Untreated or TAFIa treated HMW-FDPs were titrated stepwise into 100 nM 5IAF-Glu-Pg or 5IAF-Lys-Pg until the fluorescence change saturated. Ligand solutions were supplemented with 100 nM 5IAF-Pg to avoid dilution effects. All titrations were performed in HBST. The fractional fluorescence change from each titration was analyzed by non-linear regression to Equation 1.

$$\frac{I}{I_o} = I_{blank} + (r-1)\frac{1}{2[\mathrm{P}]_o}\left(K_P + [\mathrm{P}]_o + [\mathrm{F}]_o - \sqrt{(K_P + [\mathrm{P}]_o + [\mathrm{F}]_o)^2 - 4[\mathrm{P}]_o[\mathrm{F}]_o}\right) \quad \text{(Eq. 1)}$$

where I/I_o is the measured fractional fluorescence change, r is the ratio of the fluorescence coefficients for 5IAF-Pg in the bound and free states, $[\mathrm{P}]_o$ and $[\mathrm{F}]_o$ are the total Pg and HMW-FDP concentrations respectively, and K_P is the dissociation constant of Pg for the HMW-FDPs. I_{blank} is the fractional fluorescence change at 0 nM HMW-FDPs as determined by the fit to the data.

Measuring the Rate of 5IAF-Pg Cleavage – 5IAF-Pg cleavage was monitored by fluorescein fluorescence in a Spectramax Gemini XS fluorescence plate reader

(Molecular Devices, Sunnyvale, CA). Fluorescein was excited at 490 nm and emission was detected at 535 nm with a 530 nm emission cutoff filter. The opaque 96-well Microfluor plate was blocked overnight with HBS, 1% Tween 80 before use to minimize non-specific binding to the plastic. 5IAF-Glu-Pg or 5IAF-Lys-Pg (25-300 nM) was incubated with 10-300 nM untreated or TAFIa treated HMW-FDPs in HBST. 5IAF-Glu-Pg cleavage on untreated and TAFIa treated HMW-FDPs was started with 5 nM and 50 nM (final concentration) tPA respectively. 5IAF-Lys-Pg cleavage on untreated and TAFIa treated HMW-FDPs was started with 1 nM and 20 nM (final concentration) tPA respectively. The initial rates of fluorescence decrease were determined by linear regression of the first 10-15 % of the data. These rates were converted to rates of 5IAF-Pg cleavage using Equation 2.

$$\frac{d[\mathrm{P}]}{dt} = \left(\frac{dI}{dt}\right)\left(\frac{[\mathrm{P}]_o}{\Delta I[\mathrm{A}]_o}\right) \qquad \text{(Eq. 2)}$$

where $d[\mathrm{P}]/dt$ is the rate of 5IAF-Pg cleavage, dI/dt is the rate of fluorescence decrease, ΔI is the total fluorescence decrease upon 5IAF-Pg cleavage, and $[\mathrm{A}]_o$ is the total activator (tPA) concentration.

The initial rate data were modeled according to the steady-state template model for Pg activation first described by Horrevoets *et al.* (31), shown in Fig. 2-1. The rate equation for this model is shown in Equation 3.

$$\frac{v}{[\mathrm{A}]_o} = \frac{k_{cat}\left(\frac{[\mathrm{F}]_o}{[\mathrm{F}]_o + K_{PA}}\right)[\mathrm{P}]_f}{K_{AP}\left(\frac{[\mathrm{F}]_o + K_A}{[\mathrm{F}]_o + K_{PA}}\right) + [\mathrm{P}]_f} \qquad \text{(Eq. 3)}$$

where k_{cat} is the turnover number, K_{AP} is the binding constant of Pg for the

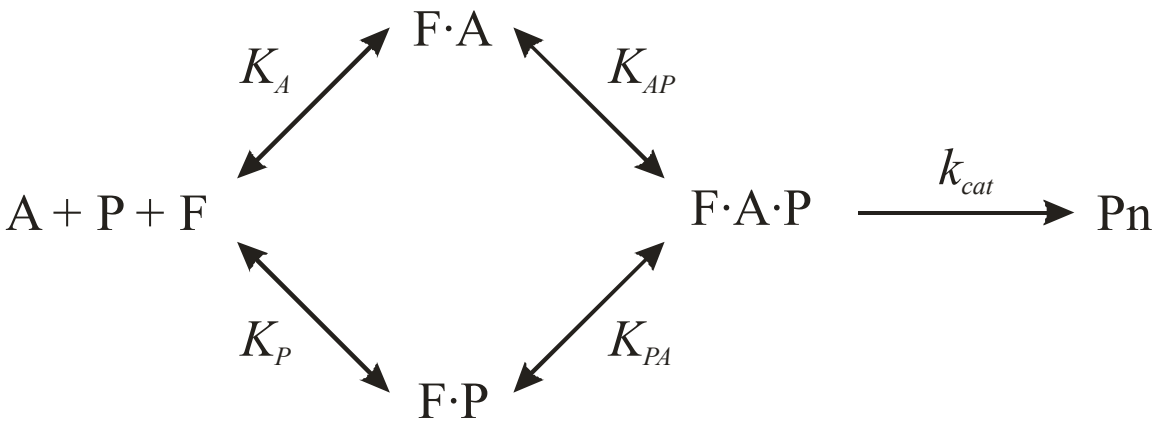

Figure 2-1. The steady state template model of Pg activation. In this model, Pg (P) and tPA (A) can each bind to the HMW-FDPs (F) forming their respective binary complexes (FP and FA), with binding constants K_P and K_A. tPA or Pg can bind to these binary complexes with binding constants K_{PA} and K_{AP} to form the ternary complex (FAP). Once formed, tPA cleaves Pg to form Pn with a rate constant k_{cat}.

activator:HMW-FDP complex, K_{PA} is the binding constant of the activator for the Pg:HMW-FDP complex, and K_A is the dissociation constant of the activator for the HMW-FDPs. $[P]_f$, the free Pg concentration, was calculated using Equation 4.

$$[P] = [P]_o - \tfrac{1}{2}\left(K_P + [P]_o + [F]_o - \sqrt{(K_P + [P]_o + [F]_o)^2 - 4[P]_o[F]_o}\right) \quad \text{(Eq. 4)}$$

Equation 3 is identical in form to the Michaelis-Menten equation, shown in equation 5.

$$\frac{v}{[A]_o} = \frac{k_{cat(app)}[P]_f}{K_{m(app)} + [P]_f} \quad \text{(Eq. 5)}$$

where $k_{cat(app)}$ and $K_{m(app)}$ are the apparent k_{cat} and K_m and given by Equations 6 and 7.

$$k_{cat(app)} = k_{cat}\left(\frac{[F]_o}{[F]_o + K_{PA}}\right) \quad \text{(Eq. 6)}$$

$$K_{m(app)} = K_{AP}\left(\frac{[F]_o + K_A}{[F]_o + K_{PA}}\right) \quad \text{(Eq. 7)}$$

Thus, the apparent k_{cat}/K_m, $k_{cat(app)}/K_{m(app)}$, is given by Equation 8.

$$\frac{k_{cat(app)}}{K_{m(app)}} = \left(\frac{k_{cat}}{K_{AP}}\right)\left(\frac{[F]_o}{[F]_o + K_A}\right) \quad \text{(Eq. 8)}$$

First, the rates of 5IAF-Pg cleavage at each HMW-FDP concentration were fit by nonlinear regression to the Michaelis-Menten equation (Equation 5) to obtain the $k_{cat(app)}/K_{m(app)}$. $k_{cat(app)}/K_{m(app)}$ was plotted against [HMW-FDPs] and fit by nonlinear regression to Equation 8 to determine k_{cat}/K_{AP} and K_A. With K_A, the data for each condition was globally fit to Equation 3 to yield values for k_{cat}, K_{PA}, and K_{AP}.

Because the rates of 5IAF-Glu-Pg cleavage on TAFIa treated HMW-FDPs did not show saturation, the $K_{m(app)}$ was assumed to be much larger than $[P]_f$. Under this assumption, Equation 5 simplifies to Equation 9, which was used to obtain $k_{cat(app)}/K_{m(app)}$.

$$\frac{v}{[A]_o} = \frac{k_{cat(app)}}{K_{m(app)}}[P]_f \quad \text{(Eq. 9)}$$

Determination of the Free Pn Concentration, the Residual AP Concentration, the Rate of Pn Formation, and the Second Order Rate Constant for Pn Inhibition by AP in Real Time – The free Pn concentration, the residual AP concentration, the rate of Pn formation, and the k_2 for Pn inhibition by AP were determined as previously described (47). Briefly, identical clots (120 μL) were formed by adding 5 nM thrombin to 4 μM Fg, 500 nM Glu- or Lys-Pg, 500 nM 5IAF-Glu- or 5IAF-Lys-Pg, 500 nM AP, 0-0.5 nM TAFIa, 5 mM $CaCl_2$, 400 μM S2251, and 2 nM tPA. In these experiments, hirudin was not added to inhibit the thrombin after the TAFI was activated as described above under *TAFIa Treated HMW-FDP Production.* The clots formed in a clear 96-well plate were monitored by absorbance at 405 and 650 nm simultaneously in a Spectramax Plus plate reader (Molecular Devices, Sunnyvale, CA). Absorbance at 405 nm detected clotting and S2251 hydrolysis, while absorbance at 650 nm detected clotting alone. After subtracting out the absorbance due to clotting, the free Pn concentration, $[Pn]_f$, was determined using Equation 10.

$$[Pn]_f = \left(1 - \left(\frac{[S2251]}{[S2251]_o + K_S}\right)\right)[Pn] \quad \text{(Eq. 10)}$$

where K_S is the K_m for S2251 hydrolysis (102.5 μM) and [Pn] is the total Pn present. [Pn] was determined using a standard curve in which clots were formed with known amounts of Pn in the absence of AP.

The clots formed in an opaque 96-well plate were in a Spectramax Gemini XS fluorescence plate reader. Fluorescein was excited at 490 nm and emission was detected at 535 nm with a 530 nm emission cutoff filter. The rate of Pn formation, r_{form}, was

calculated using Equation 2 except that the rate of fluorescence decay was not divided by the enzyme concentration, which yielded a rate in nM/s rather than s^{-1}. The residual AP concentration, [AP], was determined using Equation 11.

$$[\mathrm{AP}] = [\mathrm{AP}]_o - [\mathrm{P}]_o + [\mathrm{P}]_o \left(\frac{I - I_f}{I_o - I_f} \right) \qquad \text{(Eq. 11)}$$

where $[\mathrm{AP}]_o$ is the total AP concentration, I is the measured fluorescence at any time, I_o and I_f are the initial and final fluorescence values respectively. Lastly, the k_2 for Pn inhibition by AP was calculated using Equation 12.

$$k_2 = \frac{r_{\mathrm{form}}}{[\mathrm{AP}][\mathrm{Pn}]_f} \qquad \text{(Eq. 12)}$$

PAI-1 Activity Assay – Because PAI-1 spontaneously converts from an active to a latent conformation, the concentration of active PAI-1 was determined. 5 nM (final concentration) tc-tPA was incubated with 0-10 nM (final concentration) PAI-1 in HBST for 30 min at 25ºC. The residual tPA activity was measured by adding 400 μM (final concentration) S2765, a chromogenic substrate specific for tPA. The initial rate of S2765 hydrolysis was plotted versus the PAI-1 concentration. The PAI-1 concentration capable of inhibiting 5 nM tc-tPA was determined by linear regression of the non-zero data points in SigmaPlot (Systat Software Inc., Point Richmond CA) and calculating the x-intercept. The PAI-1 concentration was then corrected for its activity, which was typically 90-95%. The PAI-1 concentration reported in all further assays is the active concentration.

End Point Method for Monitoring tPA Inhibition by PAI-1 – A previously devised end point assay (65,69) was used to study tPA inhibition by PAI-1 in the presence of HMW-FDPs. When tPA and a corresponding chromogenic substrate are mixed, the reaction, monitored by absorbance, goes to completion due to depletion of the substrate.

If PAI-1 is present in excess over tPA, the reaction stops before complete substrate hydrolysis due to tPA inactivation. The reaction mechanism is shown in Fig. 2-2, where A is the activator (tPA), S is the substrate (S2765), I is the inhibitor (PAI-1), K_S is the K_m for tPA and S2765 binding, and k_{cat} is the rate constant for S2765 hydrolysis by tPA.

The rate of S2765 hydrolysis by tPA is described by Equation 13.

$$\frac{d[\mathrm{S}]}{dt} = -\frac{k_{cat}[\mathrm{A}][\mathrm{S}]}{K_S} \qquad \text{(Eq. 13)}$$

The rate of tPA inhibition by PAI-1 is given in Equation 14.

$$\frac{d[\mathrm{A\text{-}I}]}{dt} = \frac{k_2([\mathrm{I}]_o - [\mathrm{A\text{-}I}])[\mathrm{A}]}{K_S} \qquad \text{(Eq. 14)}$$

After solving for [A] in both expressions, Equations 13 and 14 can be combined as Equation 15.

$$\frac{d[\mathrm{S}]}{[\mathrm{S}]}\frac{K_S}{k_{cat}}k_2 = -\frac{d[\mathrm{A\text{-}I}]}{[\mathrm{I}]_o - [\mathrm{A\text{-}I}]} \qquad \text{(Eq. 15)}$$

Integrating both sides of Equation 15 results in Equation 16.

$$\ln\left(\frac{[\mathrm{S}]}{[\mathrm{S}]_o}\right)\frac{K_S}{k_{cat}}k_2 = \ln\left(\frac{[\mathrm{I}]_o - [\mathrm{A\text{-}I}]}{[\mathrm{I}]_o}\right) \qquad \text{(Eq. 16)}$$

Provided [I] is greater than [A] and the rate of substrate hydrolysis is small compared to inhibition, the reaction will stop before complete substrate hydrolysis due to tPA inactivation. At the end of the reaction, the final A-I complex concentration is equal to the input enzyme concentration. Therefore, k_2 can be determined using Equation 17 by measuring the substrate concentration at the end of the reaction.

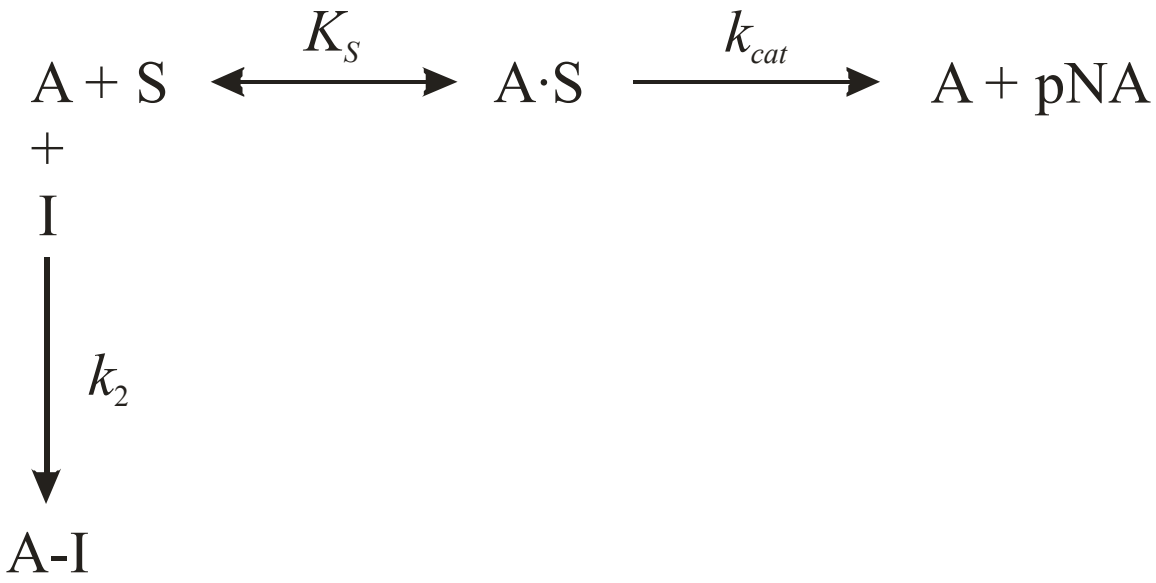

Figure 2-2. The Endpoint Model to Measure tPA Inhibition by PAI-1. In this model, tPA (A) can bind and subsequently cleave the substrate (S), with respective Michaelis (K_S) and catalytic (k_{cat}) constants. tPA can also be irreversibly inhibited by PAI-1 (I) with the apparent second order inhibition rate constant k_2. The reaction is measured by absorbance and the endpoint is used to determine k_2.

$$k_2 = \frac{\ln\left(1 - \frac{[A]_o}{[I]_o}\right)}{\ln\left(\frac{[S]_f}{[S]_o}\right)} \frac{k_{cat}}{K_S} \qquad \text{(Eq. 17)}$$

In the end point assay, $[S]_o$ is determined by measuring the change in absorbance at the end of a reaction in the absence of PAI-1; $[S]_f$ is determined by the difference in absorbance at the end of the reaction in the presence and absence of PAI-1.

k_{cat} and K_S Determination – As shown in Equation 17, k_{cat} and K_S must be known in order to calculate k_2. To determine these values, 0-800 μM (final concentration) S2765 was hydrolyzed with 5 nM (final concentration) tPA or tc-tPA in the presence of 0-100 nM (final concentration) HMW-FDPs in HBST at 25°C. The reaction was monitored by absorbance at 405 nm in a Spectramax Plus absorbance plate reader (Molecular Devices, Sunnyvale, CA). The initial rates of S2765 hydrolysis, determined using the Spectramax software, SoftMax Pro, were converted to moles of product formed per second per mole of enzyme and plotted *versus* the initial S2765 concentration. The k_{cat} and K_S values at each HMW-FDP concentration were determined by non-linear regression to the Michaelis-Menten equation in SigmaPlot. The k_{cat}/K_S values displayed a HMW-FDP dependent non-linear increase for tPA mediated S2765 hydrolysis. The k_{cat}/K_S values were plotted versus HMW-FDP concentration and the data was fit to a three parameter hyperbolic function in SigmaPlot. The k_{cat}/K_S values predicted by the fit were used to calculate k_2 at each HMW-FDP concentration. No such increase was observed with tc-tPA; thus, the k_{cat}/K_S values were averaged and this value was used for all HMW-FDP concentrations.

Measuring the Effect of Vitronectin on k_2 – The end point assay was used to calculate

k_2 as a function of the vitronectin (Vn) concentration in the presence and absence of 100 nM HMW-FDPs. Vn (0-500 nM) was incubated with 400 μM S2765, with or without 10 nM PAI-1 in HBST. The reaction was initiated by addition of 5 nM (final concentration) tPA and monitored in a Spectramax Plus absorbance plate reader at 405 nm. The endpoint of the reaction was subtracted from the blank (no tPA) and used to calculate k_2 with Equation 17.

Measuring the Effect of Untreated and TAFIa Treated HMW-FDPs on k_2 – The end point assay was used to calculate k_2 as a function of HMW-FDPs. Untreated or TAFIa treated HMW-FDPs (0-100 nM) were incubated with 400 μM S2765, with or without 200nM Vn, and 10 nM PAI-1 in HBST. The reaction was initiated by addition of 5 nM (final concentration) tPA or tc-tPA and monitored in a Spectramax Plus absorbance plate reader at 405 nm. The endpoint of the reaction was subtracted from the blank (no tPA) and used to calculate k_2 with Equation 17.

End Point Method for Monitoring tPA Inhibition by PAI-1 in the Presence of 5IAF-Pg – The end point method was used with 5IAF-Pg as the substrate to quantify the effect of Pg on tPA inhibition by PAI-1. The model of Pg activation is shown in Fig. 2-3, where P is 5IAF-Pg, F is the HMW-FDPs, A is the activator (tPA), K_A and K_P are the dissociation constants for tPA and 5IAF-Pg binding to HMW-FDPs, and K_{PA} and K_{AP} are the binding constants for tPA and 5IAF-Pg binding to the respective binary complexes. The rate of Pg cleavage is given by Equation 18.

$$\frac{d[\mathrm{P}]_o}{dt} = -\frac{k_{cat}[\mathrm{F}][\mathrm{A}][\mathrm{P}]_o}{K_A K_{AP}\left(1+\frac{[\mathrm{F}]}{K_P}\right)} \qquad \text{(Eq. 18)}$$

where $[\mathrm{P}]_o$ is the total Pg concentration and [F] and [A] are the free HMW-FDP and free

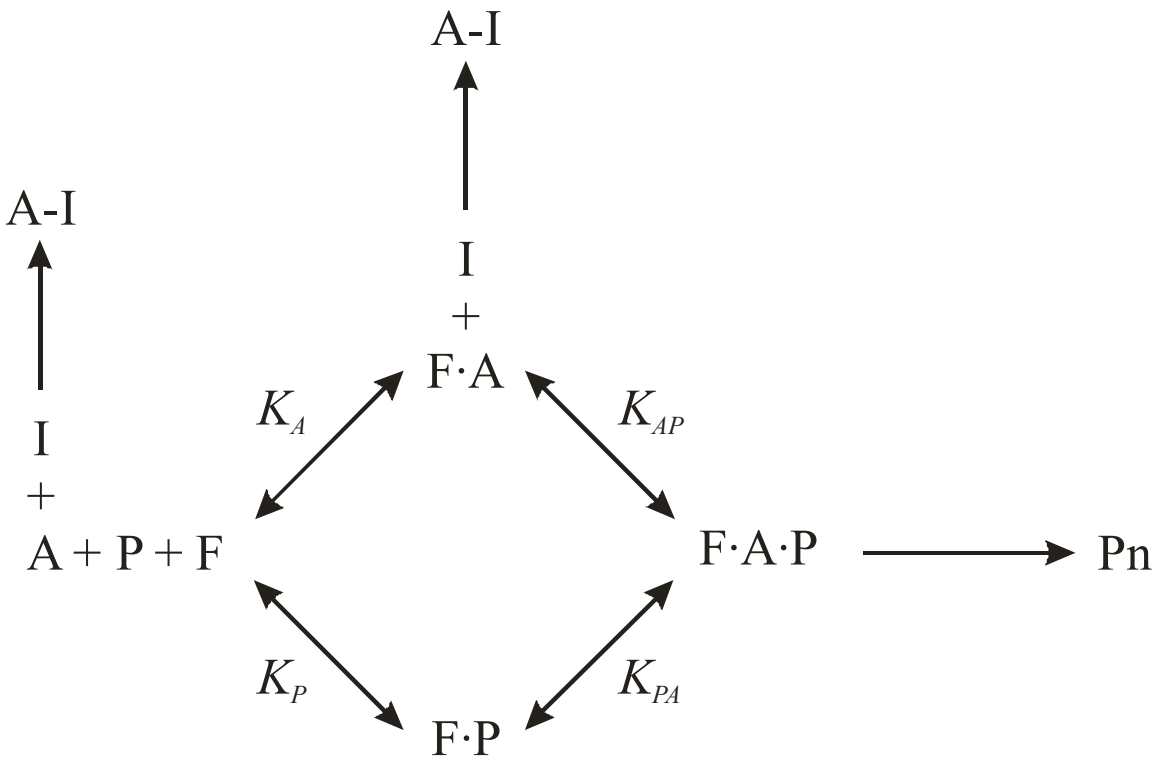

Figure 2-3. The Endpoint Model Used to Measure tPA Inhibition in the Presence of Pg. In this model, Pg (P) and tPA (A) can each bind to the HMW-FDPs (F) forming their respective binary complexes (FP and FA), with dissociation constants K_P and K_A. tPA or Pg can bind to these binary complexes with binding constants K_{PA} and K_{AP} to form the ternary complex (FAP). Once formed, tPA cleaves Pg to form Pn. PAI-1 can irreversibly inhibit tPA in solution or bound to the HMW-FDPs. The reaction is measured by fluorescence and the apparent second order inhibition rate constant is determined using the endpoint.

tPA concentrations respectively. The rate of tPA consumption is given by Equation 19.

$$\frac{d[\text{A-I}]}{dt} = k_2([\text{I}]_o - [\text{A-I}])[\text{A}] \qquad \text{(Eq. 19)}$$

Because [A] is a common factor in both expressions, Equation 19 can be rearranged to isolate [A] and the result was inserted into Equation 18, producing Equation 20.

$$\frac{d[\text{P}]_o}{[\text{P}]_o} = -\left(\frac{k_{cat}[\text{F}]}{k_2 K_A K_{AP}\left(1+\frac{[\text{F}]}{K_P}\right)}\right)\frac{d[\text{A-I}]}{[\text{I}]_o - [\text{A-I}]} \qquad \text{(Eq. 20)}$$

After integration, an expression for k_2 is obtained, shown in Equation 21.

$$k_2 = \left(\frac{k_{cat}[\text{F}]}{K_A K_{AP} + K_{PA}[\text{F}]}\right)\frac{\ln\left(\frac{[\text{I}]_o}{[\text{I}]_o - [\text{A-I}]}\right)}{\ln\left(\frac{[\text{P}]_o}{[\text{P}]_f}\right)} \qquad \text{(Eq. 21)}$$

[F] was calculated using Equation 22.

$$[\text{F}] = [\text{F}]_o - \tfrac{1}{2}\left(K_P + [\text{P}]_o + [\text{F}]_o - \sqrt{(K_P + [\text{P}]_o + [\text{F}]_o)^2 - 4[\text{P}]_o[\text{F}]_o}\right) \qquad \text{(Eq. 22)}$$

In this assay, $[\text{P}]_o$ and $[\text{P}]_f$ are determined in the same fashion as $[\text{S}]_o$ and $[\text{S}]_f$ in the chromogenic endpoint assay. The parameters k_{cat}, K_A, K_{AP}, and K_{PA} were determined from the initial rate data in the absence of PAI-1 as described above in *Measuring the Rate of 5IAF-Pg Cleavage*.

Measuring the Effect of 5IAF-Pg on k_2 – The endpoint assay was used to calculate k_2 as a function of 5IAF-Pg at various HMW-FDP concentrations. 5IAF-Pg (0-100 nM) was incubated with 25 and 50 nM HMW-FDPs and 10 nM PAI-1 or 75 and 100 nM HMW-FDPs and 15 nM PAI-1 in HBST. In each case, the Vn concentration used was 200 nM. The reaction was started by addition of 5 nM (final concentration) tPA or tc-

tPA and monitored in a Spectramax Gemini XS fluorescence plate reader with a 490 nm excitation wavelength, a 535 nm emission wavelength, and a 530 nm emission cutoff filter. k_2 was calculated using Equation 21.

Because the HMW-FDPs lose their cofactor activity upon TAFIa treatment and can no longer support Pg activation, the previous endpoint method utilizing the chromogenic substrate S2765 was used to measure the effect of 5IAF-Pg on k_2 with TAFIa treated FDPs. 5IAF-Pg (100 nM) was incubated with 0-100 nM TAFIa treated HMW-FDPs, 10 nM PAI-1, 200nM Vn, and 400 μM S2765 in HBST. The reaction was started by addition of 5 nM (final concentration) tPA and monitored in a Spectramax Plus absorbance plate reader at 405 nm. The endpoint of the reaction was subtracted from the blank (no tPA) and used to calculate k_2 with Equation 17.

3. Results

Part 1: Lys-Pg Activation on Fibrin

5IAF-Pg Binding to HMW-FDPs – Because 5IAF-Pg displays a change in fluorescence upon binding to HMW-FDPs, this property was exploited to measure the affinity of 5IAF-Glu-Pg and 5IAF-Lys-Pg for untreated and TAFIa treated HMW-FDPs (Fig. 3-1). The fluorescence changes as a function of HMW-FDP concentration were fit by nonlinear regression to Equation 1. 5IAF-Glu-Pg bound to untreated and TAFIa treated HMW-FDPs with K_ds of 127 and 645 nM respectively; 5IAF-Lys-Pg bound to the same HMW-FDPs with affinities of 1.35 and 23.3 nM respectively.

TAFIa Treatment of HMW-FDPs Decreases the Rate of 5IAF-Glu-Pg and 5IAF-Lys-Pg Cleavage – Both untreated and TAFIa treated HMW-FDPs were used respectively as models for Pn and TAFIa modified Fn to investigate tPA mediated Glu- and Lys-Pg activation. The initial rates of 5IAF-Glu- and 5IAF-Lys-Pg cleavage at each HMW-FDP concentration were fit by nonlinear regression to the Michaelis-Menten equation in terms of free Pg (Eq. 5). The parameters $k_{cat(app)}$, $K_{m(app)}$, and $k_{cat(app)}/K_{m(app)}$ derived from the fit are displayed in Tables 3-1 and 3-2. tPA mediated 5IAF-Pg cleavage exhibits Michaelis-Menten kinetics at any HMW-FDP concentration when the 5IAF-Pg concentration is expressed as its free form. The $k_{cat(app)}$ and $k_{cat(app)}/K_{m(app)}$ both increased with increasing HMW-FDPs, observations that are consistent with a template mechanism. The $K_{m(app)}$ decreased 2-3 fold for 5IAF-Pg cleavage on untreated HMW-FDPs; for 5IAF-Lys-Pg cleavage on TAFIa treated HMW-FDPs the $K_{m(app)}$ decreased approximately 10 fold. In both cases, the decrease is consistent with $K_A > K_{PA}$. The parameters $k_{cat(app)}$ and $K_{m(app)}$ could not be determined for 5IAF-Glu-Pg cleavage on TAFIa treated HMW-FDPs

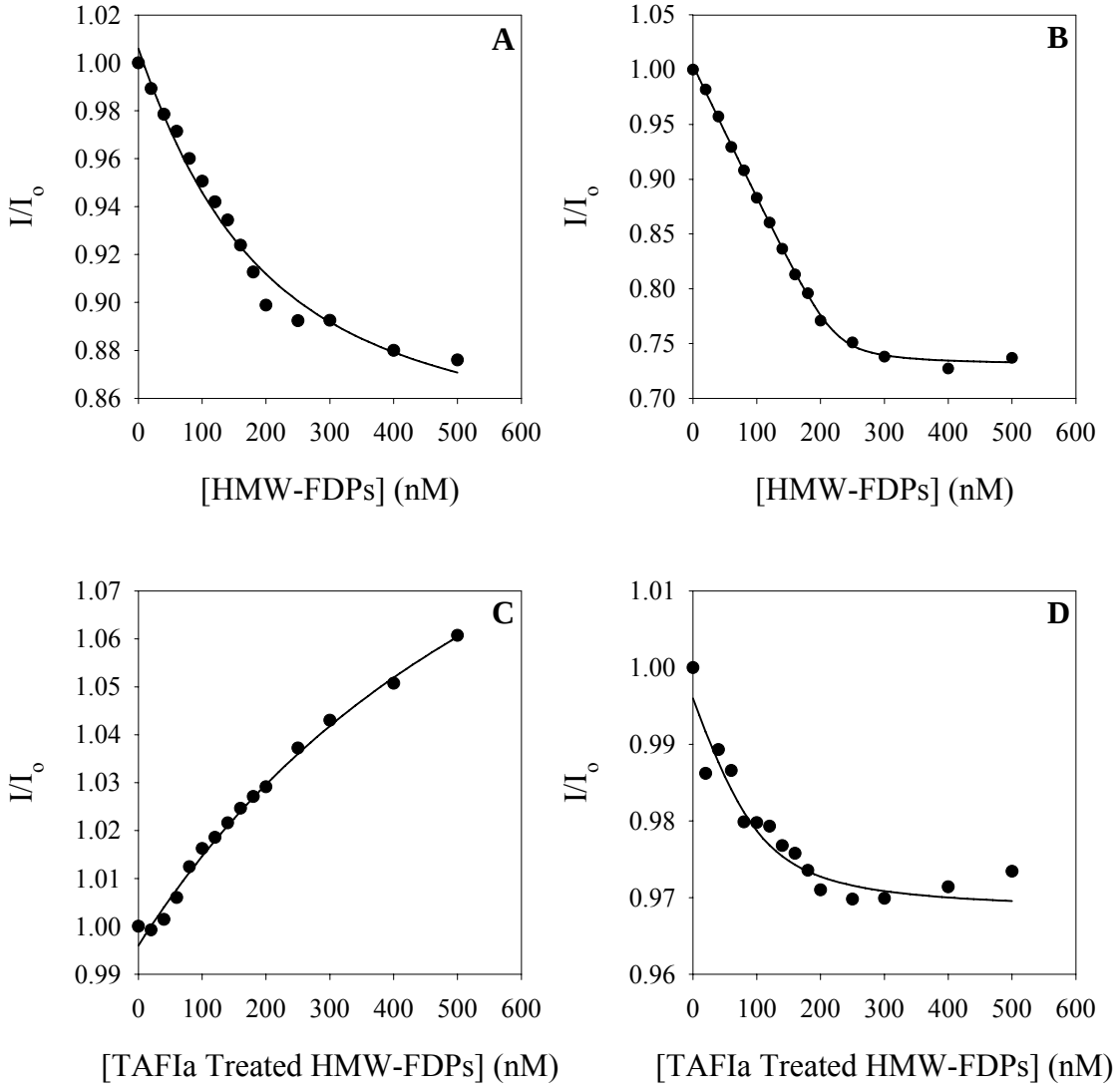

Figure 3-1. 5IAF-Glu- and 5IAF-Lys-Pg binding to untreated and TAFIa treated HMW-FDPs. The fractional fluorescence changes upon 5IAF-Glu-Pg binding to HMW-FDPs (*A*) and TAFIa treated HMW-FDPs (*C*) and 5IAF-Lys-Pg binding to HMW-FDPs (*B*) and TAFIa treated HMW-FDPs (*D*) are shown. In each case, the dissociation constant, K_P, was determined by nonlinear regression to Equation 1.

Table 3-1. The apparent k_{cat}, K_m, and k_{cat}/K_m of tPA mediated 5IAF-Glu-Pg cleavage on untreated and TAFIa treated HMW-FDPs. The rate of 5IAF-Glu-Pg cleavage at each HMW-FDP concentration was fit to the Michaelis-Menten equation in terms of free Pg (Eq. 5) by nonlinear regression to determine the $k_{cat(app)}$ and the $K_{m(app)}$, shown ± S.E.M as given by the regression algorithm. These parameters could not be determined for 5IAF-Glu-Pg cleavage on TAFIa treated HMW-FDPs. Thus, the $k_{cat(app)}/K_{m(app)}$ was determined by nonlinear regression to the Michaelis-Menten equation assuming Km>>[P] (Eq. 9). ND indicates not determined.

[HMW-FDPs] (nM)	Untreated HMW-FDPs			TAFIa Treated HMW-FDPs		
	$k_{cat(app)}$ (s^{-1})	$K_{m(app)}$ (nM)	$k_{cat(app)}/K_{m(app)}$ ($\mu M^{-1}s^{-1}$)	$k_{cat(app)}$ (s^{-1})	$K_{m(app)}$ (nM)	$k_{cat(app)}/K_{m(app)}$ ($\mu M^{-1}s^{-1}$)
25	0.009 ± 0.001	24.4 ± 8.9	0.38	ND	ND	0.0053
50	0.012 ± 0.001	15.3 ± 3.9	0.78	ND	ND	0.0087
75	0.020 ± 0.001	31.7 ± 3.3	0.62	ND	ND	0.0116
100	0.024 ± 0.001	26.2 ± 3.2	1.25	ND	ND	0.0139
150	0.029 ± 0.001	19.3 ± 3.6	1.50	ND	ND	0.0163
200	0.028 ± 0.001	9.7 ± 9.1	2.86	ND	ND	0.0166
300	0.031 ± 0.001	11.2 ± 1.4	2.75	ND	ND	0.0197

Table 3-2. The apparent k_{cat}, K_m, and k_{cat}/K_m of tPA mediated 5IAF-Lys-Pg cleavage on untreated and TAFIa treated HMW-FDPs. The rate of 5IAF-Lys-Pg cleavage at each HMW-FDP concentration was fit to the Michaelis-Menten equation in terms of free Pg (Eq. 5) by nonlinear regression to determine the $k_{cat(app)}$ and the $K_{m(app)}$, shown ± S.E.M as given by the regression algorithm. ND indicates not determined.

[HMW-FDPs] (nM)	Untreated HMW-FDPs			TAFIa Treated HMW-FDPs		
	$k_{cat(app)}$ (s^{-1})	$K_{m(app)}$ (nM)	$k_{cat(app)}/K_{m(app)}$ ($\mu M^{-1}s^{-1}$)	$k_{cat(app)}$ (s^{-1})	$K_{m(app)}$ (nM)	$k_{cat(app)}/K_{m(app)}$ ($\mu M^{-1}s^{-1}$)
25	0.019 ± 0.001	0.415 ± 0.297	47	0.003 ± 0.000	80.1 ± 19.1	0.38
50	0.028 ± 0.001	0.300 ± 0.135	95	0.004 ± 0.000	43.8 ± 10.4	0.78
75	0.039 ± 0.001	0.377 ± 0.098	103	0.006 ± 0.000	42.7 ± 8.6	0.62
100	0.043 ± 0.001	0.362 ± 0.095	117	0.008 ± 0.001	32.5 ± 6.1	1.25
150	0.042 ± 0.001	0.163 ± 0.032	259	0.010 ± 0.000	17.3 ± 1.7	1.50
200	ND	ND	ND	0.015 ± 0.001	12.3 ± 2.1	2.86
300	ND	ND	ND	0.015 ± 0.001	7.6 ± 1.0	2.75

because these reactions did not show saturation.

Since nonlinear regression of the data at all 5IAF-Pg (Glu- or Lys-Pg) and HMW-FDP (untreated or TAFIa treated) concentrations could not fit all four parameters (k_{cat}, K_A, K_{PA}, and K_{AP}) simultaneously, nonlinear regression was used to determine K_A from the $k_{cat(app)}/K_{m(app)}$ values at increasing HMW-FDP concentrations. By inputting a value for K_A into the global analysis, the other three parameters (k_{cat}, K_{PA}, and K_{AP}) were determined (Table 3-3). The solid lines shown in Fig. 3-2 are the fits to the data determined by this regression analysis. The analysis showed that TAFIa decreases the rate of both 5IAF-Glu- and 5IAF-Lys-Pg cleavage, mostly a result of an increase in the K_m. TAFIa decreased for 5IAF-Glu-Pg cleavage by 417-fold and the k_{cat}/K_m for 5IAF-Lys-Pg cleavage by 55-fold. In short, TAFIa suppresses 5IAF-Glu-Pg cleavage 7.6 times more than 5IAF-Lys Pg cleavage.

Part 2: Lys-Pn Protection from AP by Fibrin

TAFIa Prolongs Lysis in the Presence of Lys-Pg – Although Bajzar *et al.* (52) observed no TAFI dependent prolongation of lysis in the presence of Lys-Pg, TAFIa not only prolonged the lysis of purified clots containing Glu-Pg, but also those containing Lys-Pg. 500 pM TAFIa prolonged lysis by 123 min in the presence of Glu-Pg and by 75 min in the presence of Lys-Pg (Fig. 3-3).

TAFIa Attenuates the Protection of Glu-Pn But Not Lys-Pn From Inhibition By AP – Clots formed by adding thrombin to Fg, Pg, AP, and tPA contained S2251, a chromogenic Pn substrate, and 5IAF-Pg to quantify the rate of Pn inhibition by AP during clotting and subsequent lysis. Identical clots were monitored by absorbance at 405 nm (detects clotting and S2251 hydrolysis) and 650 nm (measures clotting only)

Table 3-3. The kinetic parameters of tPA mediated 5IAF-Glu- and 5IAF-Lys-Pg cleavage on untreated and TAFIa treated HMW-FDPs. The rates of 5IAF-Glu- and 5IAF-Lys-Pg cleavage were fit to the steady state template model (Eq. 3) with a set K_A, determined as described under "Experimental Procedures". Values are presented as ± S.E.M. ND indicates not determined.

Constant	5IAF-Glu-Pg		5IAF-Lys-Pg	
	Untreated HMW-FDPs	TAFIa Treated HMW-FDPs	Untreated HMW-FDPs	TAFIa Treated HMW-FDPs
k_{cat} (s^{-1})	0.0428 ± 0.0022	ND	0.0595 ± 0.0048	0.0298 ± 0.0063
K_A (nM)	843 ± 687	90.9 ± 8.2	67.3 ± 40.6	406 ± 70
K_P (nM)	127 ± 32	645 ± 160	1.352 ± 0.547	23.3 ± 42.4
K_{PA} (nM)	95.4 ± 12.1	91 ± 145	48.5 ± 9.9	312 ± 312
K_{AP} (nM)	4.04 ± 2.88	ND	0.031 ± 0.011	8.51 ± 4.56
k_{cat}/K_m ($\mu M^{-1}s^{-1}$)	10.6	0.0254	192	3.5

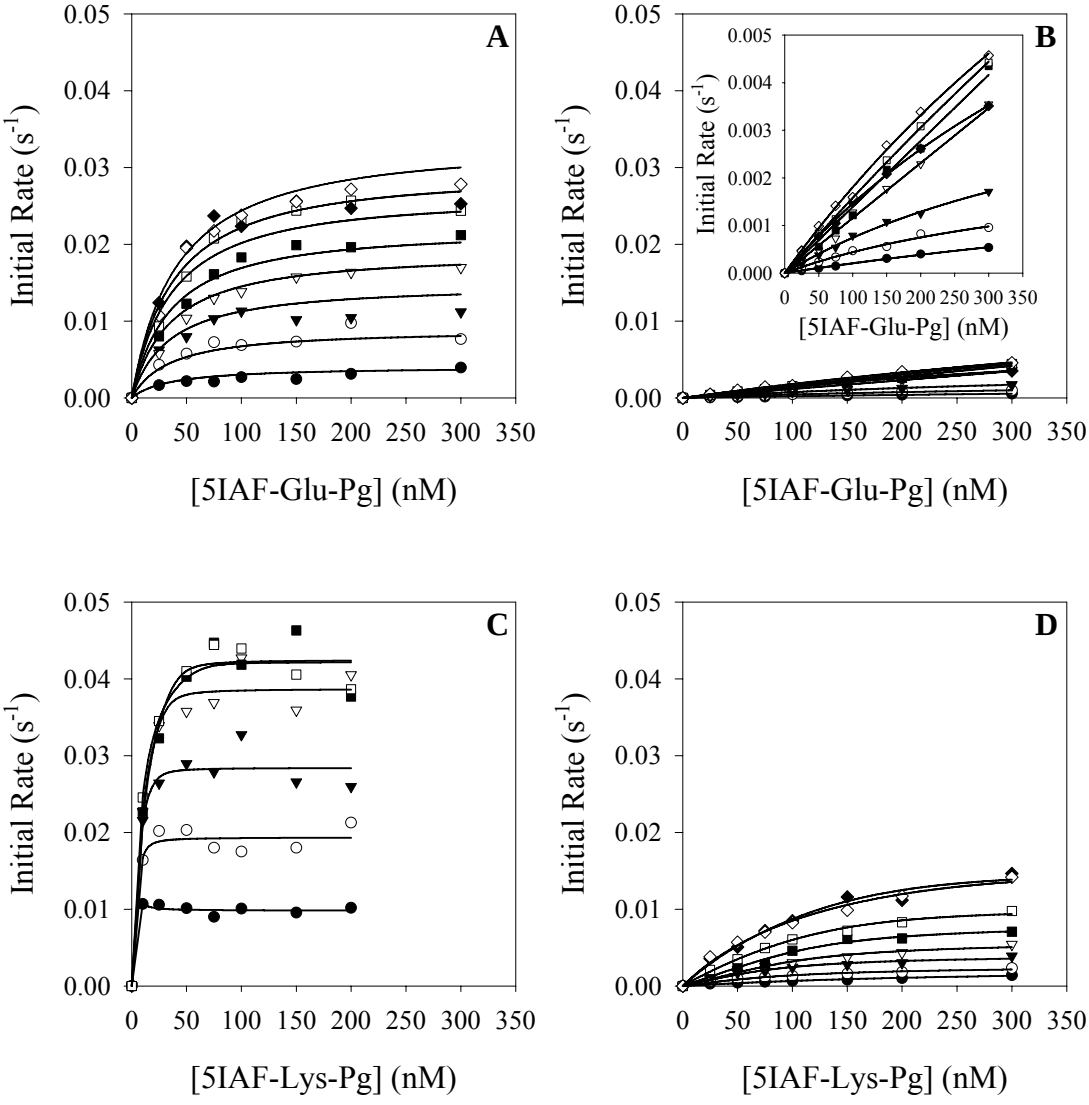

Figure 3-2. 5IAF-Glu- and 5IAF-Lys-Pg cleavage on untreated HMW-FDPs and TAFIa treated HMW-FDPs by tPA. The initial rates of 5IAF-Glu-Pg cleavage on HMW-FDPs (*A*) and TAFIa treated HMW-FDPs (*B*) and 5IAF-Lys-Pg cleavage on HMW-FDPs (*C*) and TAFIa treated HMW-FDPs (*D*) are shown. The HMW-FDP concentrations were 10 nM (*closed circles*), 25 nM (*open circles*), 50 nM (*closed triangles*), 75 nM (*open triangles*), 100 nM (*closed squares*), 150 nM (*open squares*), 200 nM (*closed diamonds*), and 300 nM (*open diamonds*). The solid lines represent the fits of the data to the steady state template model by nonlinear regression.

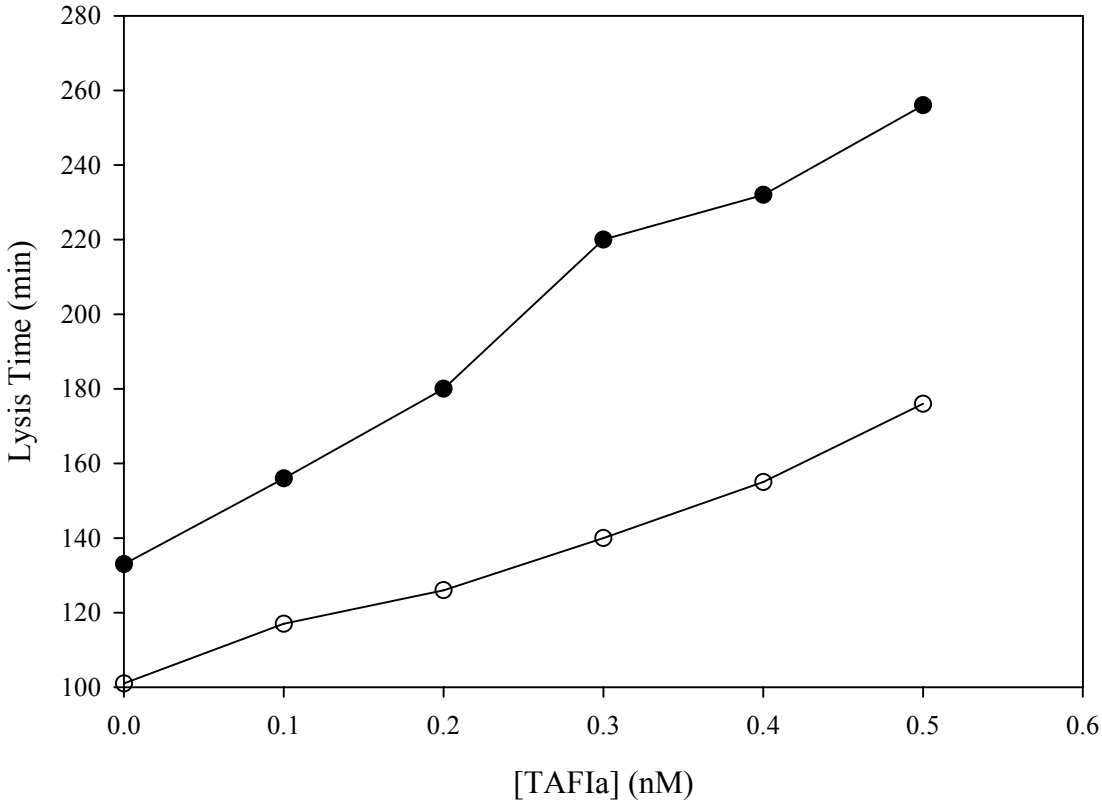

Figure 3-3. The effects of TAFIa on clot lysis in the presence of Glu-Pg or Lys-Pg. Clots formed from purified components containing either Glu- (*closed circles*) or Lys-Pg (*open circles*) were monitored by absorbance at 650 nm. The lysis time was taken as the time for the turbidity to reach 50% of its maximum.

simultaneously as well as by fluorescence to determine $[Pn]_f$, r_{form}, [AP], and k_2 over time (Fig. 3-4).

Fig. 3-5 displays the $[Pn]_f$, r_{form}, [AP], and k_2 over time in clots formed with Glu-Pg. As panel A shows, Pn levels, following a lag phase, reached a steady state, peaked during lysis, then subsided after the clot had dissolved. Both the steady state Pn level and the timing of the Pn peak were dependent on the TAFIa concentration. The steady state Pn level varied from 0.9 nM in the absence of TAFIa to 0.15 nM at 500 pM TAFIa. At each TAFIa concentration, Pn reached a maximum at 50% lysis; in other words, the peak in Pn coincided with the lysis time.

In the absence of TAFIa, k_2 rapidly decreased from 1.9×10^6 $M^{-1}s^{-1}$ to 0.2×10^6 $M^{-1}s^{-1}$, eventually reaching a minimum of 0.1×10^6 $M^{-1}s^{-1}$. Previous experiments determined that the k_2 for Pn inhibition by AP in solution was 9.6×10^6 $M^{-1}s^{-1}$ (65). Thus, Pn modified fibrin protects Pn from inhibition by an additional 10-fold over intact fibrin, a total of 50-fold over Pn inhibition in solution, which is consistent with previously published data (47). In the presence of TAFIa , k_2 was 1.6×10^6 $M^{-1}s^{-1}$ after clot formation, but the immediate drop in k_2 seen in the absence of TAFIa was delayed. Furthermore, the time elapsed before the decrease in k_2 was dependent on the TAFIa concentration.

Fig. 3-6 displays the $[Pn]_f$, r_{form}, [AP], and k_2 over time in clots formed with Lys-Pg instead of Glu-Pg. In these experiments, Pn levels quickly reached a steady state; the lag seen with Glu-Pg did not occur with Lys-Pg. The steady state Pn level was again dependent on the TAFIa concentration, ranging from 1.1 nM in the absence of TAFIa to 0.6 nM at 500 pM TAFIa. Interestingly, the difference in the steady state Pn

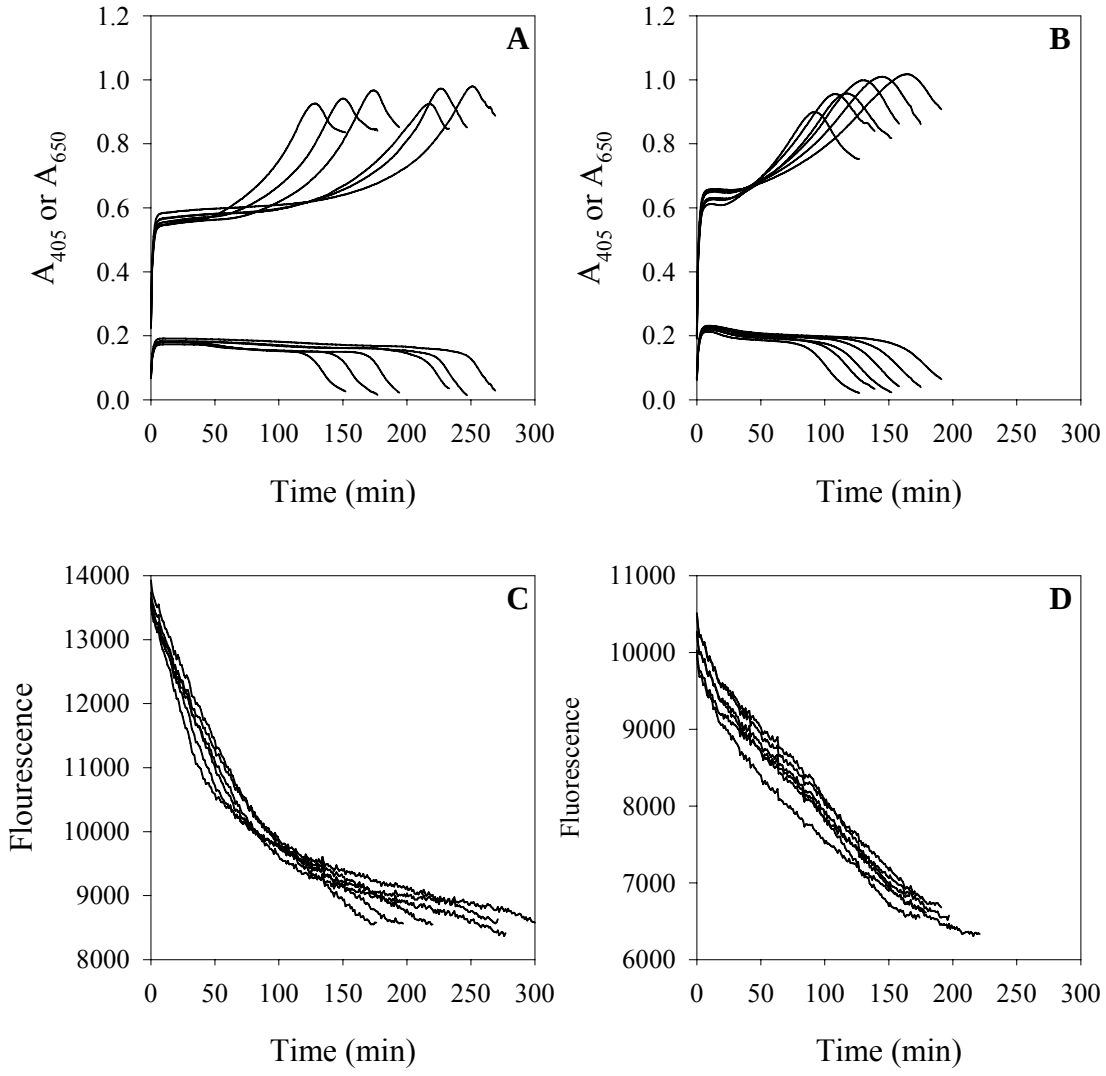

Figure 3-4. Absorbance and fluorescence time course profiles of clots in the presence of Glu- or Lys-Pg at increasing TAFIa concentrations. Clots containing either Glu- (*A*) or Lys-Pg (*B*) were monitored by absorbance at 405 (top solid lines in *A* and *B*) and 650 nm (bottom solid lines in *A* and *B*). Absorbance at 405 nm measured S2251 hydrolysis and turbidity and absorbance at 650 nm measured turbidity only. From left to right, the TAFIa concentrations were 0, 100, 200, 300, 400, and 500 pM. Identical clots containing either Glu- (*C*) or Lys-Pg (*D*) were monitored by fluorescence to measure 5IAF-Glu- and 5IAF-Lys-Pg cleavage. The TAFIa concentrations are the same as in Panels *A* and *B*. The absorbance data was used to calculate $[Pn]_f$, and the fluorescence data was used to calculate r_{form} and [AP].

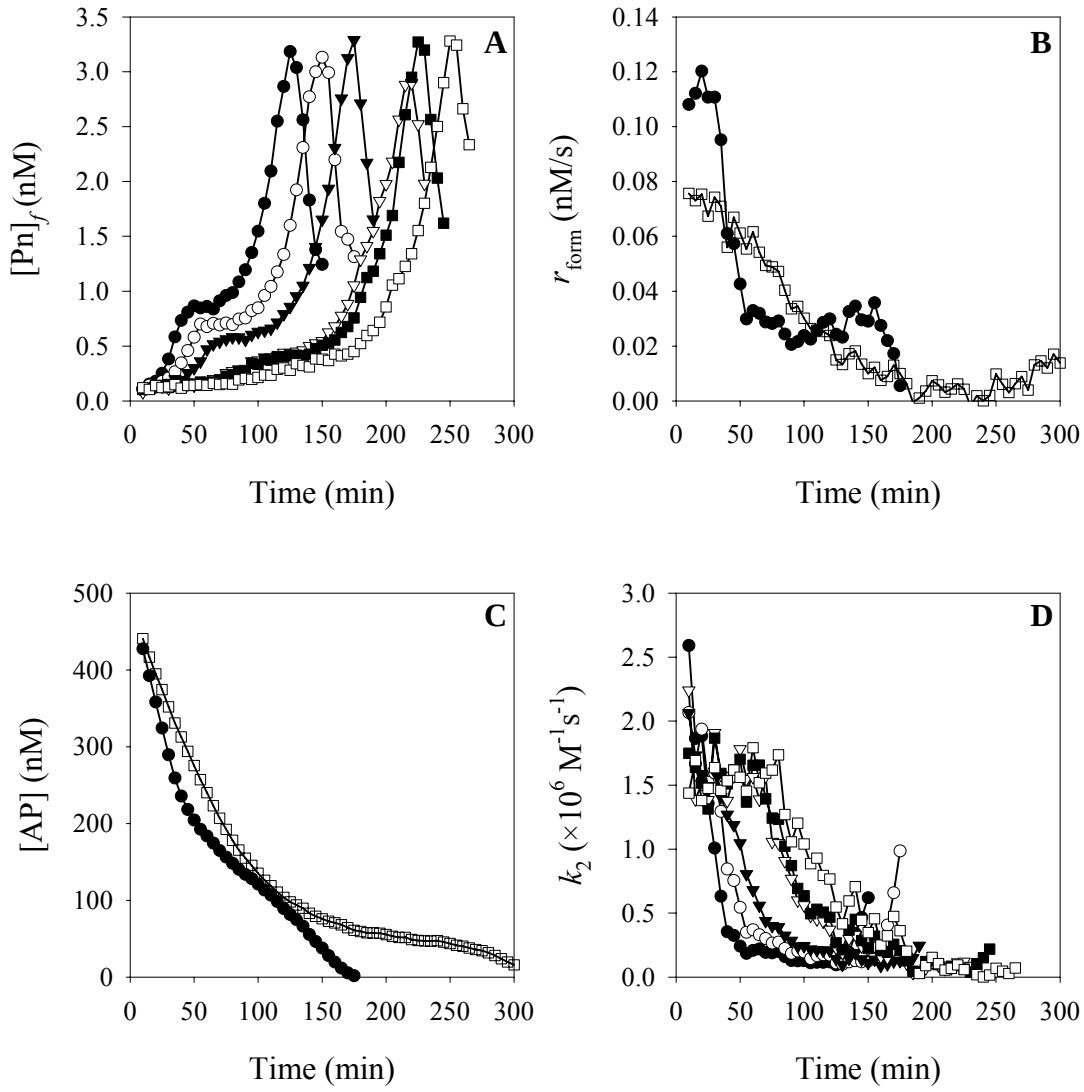

Figure 3-5. **The $[Pn]_f$, r_{form}, [AP], and k_2 for clots formed in the presence of Glu-Pg.** The absorbance and fluorescence data displayed in Figs. 3-4A and C were used to calculate $[Pn]_f$ (*A*), r_{form} (*B*), [AP] (*C*), and k_2 (*D*). The TAFIa concentrations shown are 0 pM (*closed circles*), 100 pM (*open circles*), 200 pM (*closed triangles*), 300 pM (*open triangles*), 400 pM (*closed squares*), and 500 pM (*open squares*).

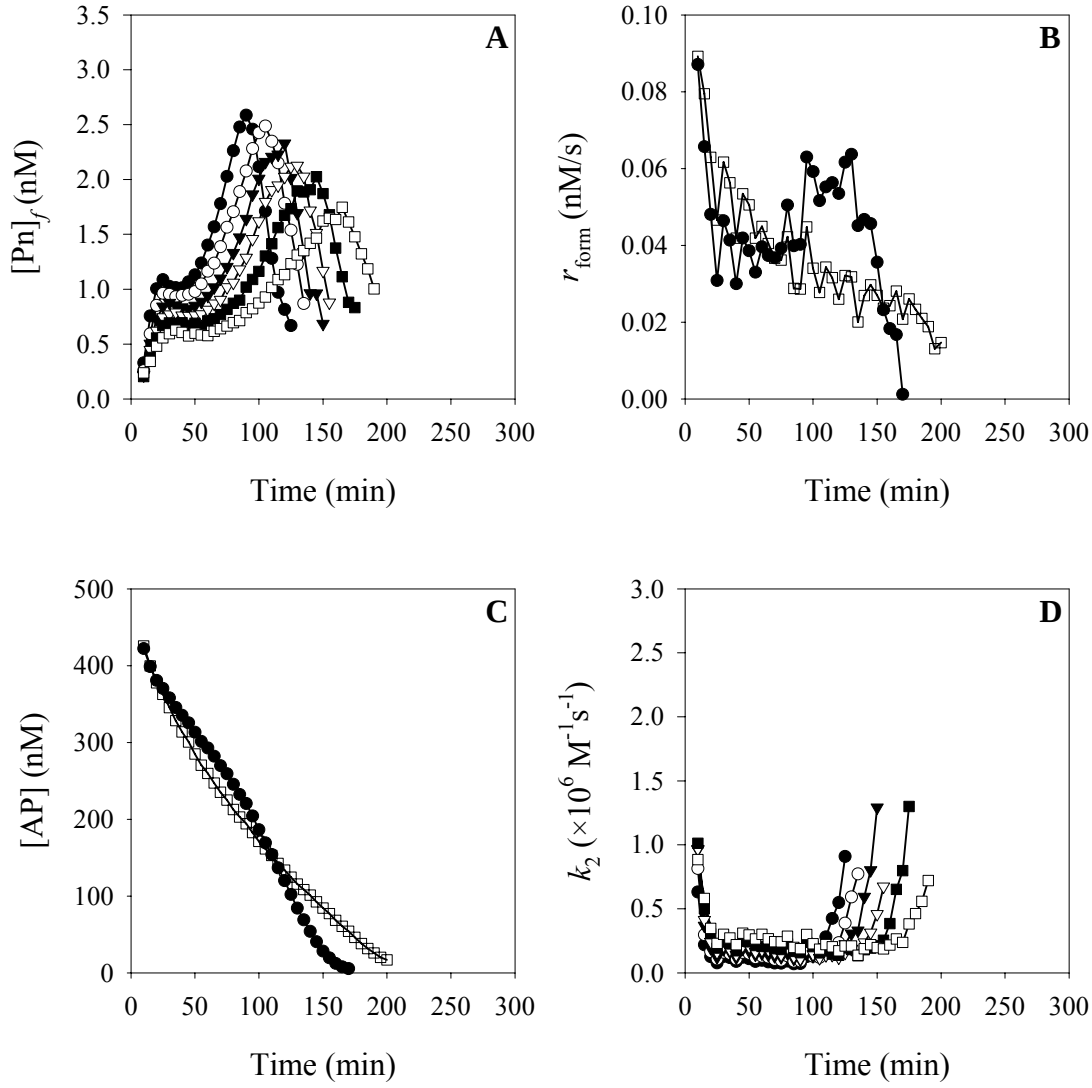

Figure 3-6. **The $[Pn]_f$, r_{form}, [AP], and k_2 for clots formed in the presence of Lys-Pg.** The absorbance and fluorescence data displayed in Figs. 3-4B and D were used to calculate $[Pn]_f$ (*A*), r_{form} (*B*), [AP] (*C*), and k_2 (*D*). The TAFIa concentrations shown are 0 pM (*closed circles*), 100 pM (*open circles*), 200 pM (*closed triangles*), 300 pM (*open triangles*), 400 pM (*closed squares*), and 500 pM (*open squares*).

concentration between Glu- and Lys-Pg increased with the TAFIa concentration. Again, a Pn peak was observed, but the maximum Pn concentration did not coincide with the lysis time. Instead, the maximum Pn concentration occurred, on average, 10 min before the lysis time. k_2, in the absence of TAFIa, rapidly decreases to 0.1×10^6 $M^{-1}s^{-1}$, similar to Glu-Pg. However, no delay was seen in the presence of TAFIa; k_2 reached a minimum for each TAFIa concentration at approximately the same time. A modest increase in k_2 was observed as the TAFIa concentration increased, rising from 0.1×10^6 $M^{-1}s^{-1}$ in the absence of TAFIa to 0.3×10^6 $M^{-1}s^{-1}$ at 500 pM TAFIa.

Part 3: tPA Protection from PAI-1 by Fibrin and Pg

PAI-1 Preferentially Inhibits tc-tPA Over sc-tPA – Due to its spontaneous latency transition, the active PAI-1 concentration was determined using tPA. Rather than the expected linear decrease in residual tPA activity with increasing PAI-1 concentration, a non-linear decrease was observed (Fig. 3-7). This observation can be explained if there are two species present and one is more active towards both the substrate and the inhibitor. Densitometry of the SDS-PAGE gel showed than approximately 10% of the tPA was in the two chain form (data not shown). To test this hypothesis, tPA was cleaved by Pn to generate tc-tPA and the PAI-1 activity assay was repeated. As expected, a linear decrease in the residual tc-tPA activity was observed. Furthermore, the initial rate of 2765 hydrolysis was higher for tc-tPA than for tPA, as seen by their respective k_{cat}/K_S values (Fig. 3-8).

Vn Has Little Effect on tPA Inhibition by PAI-1 – Previous work has indicated that Vn mediates the interaction between PAI-1 and fibrin *in vivo* (74). Endpoint assays were carried out to determine if Vn had any effect on tPA inhibition by PAI-1. In the absence

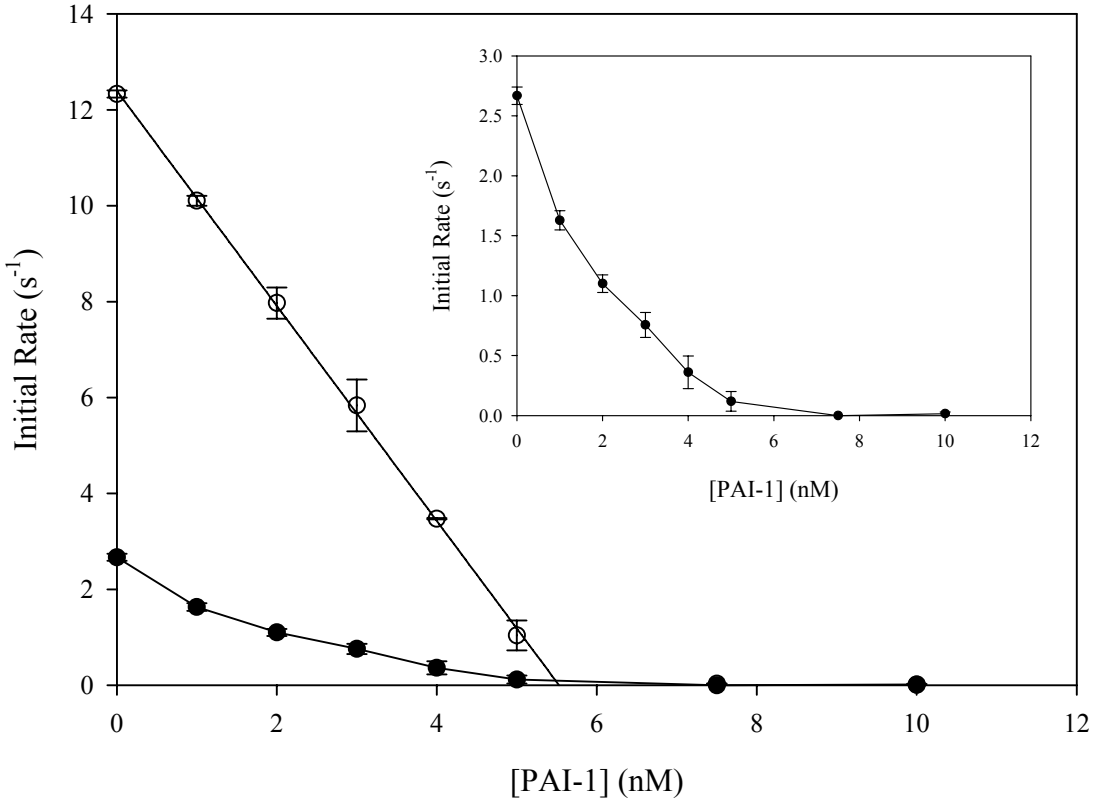

Figure 3-7. PAI-1 Activity Assay. The residual tPA (*closed circles, inset*) and tc-tPA (*open circles*) activities were measured using S2765 following inhibition by PAI-1. The tc-tPA activity from 0-5 nM was fit using linear regression as described.

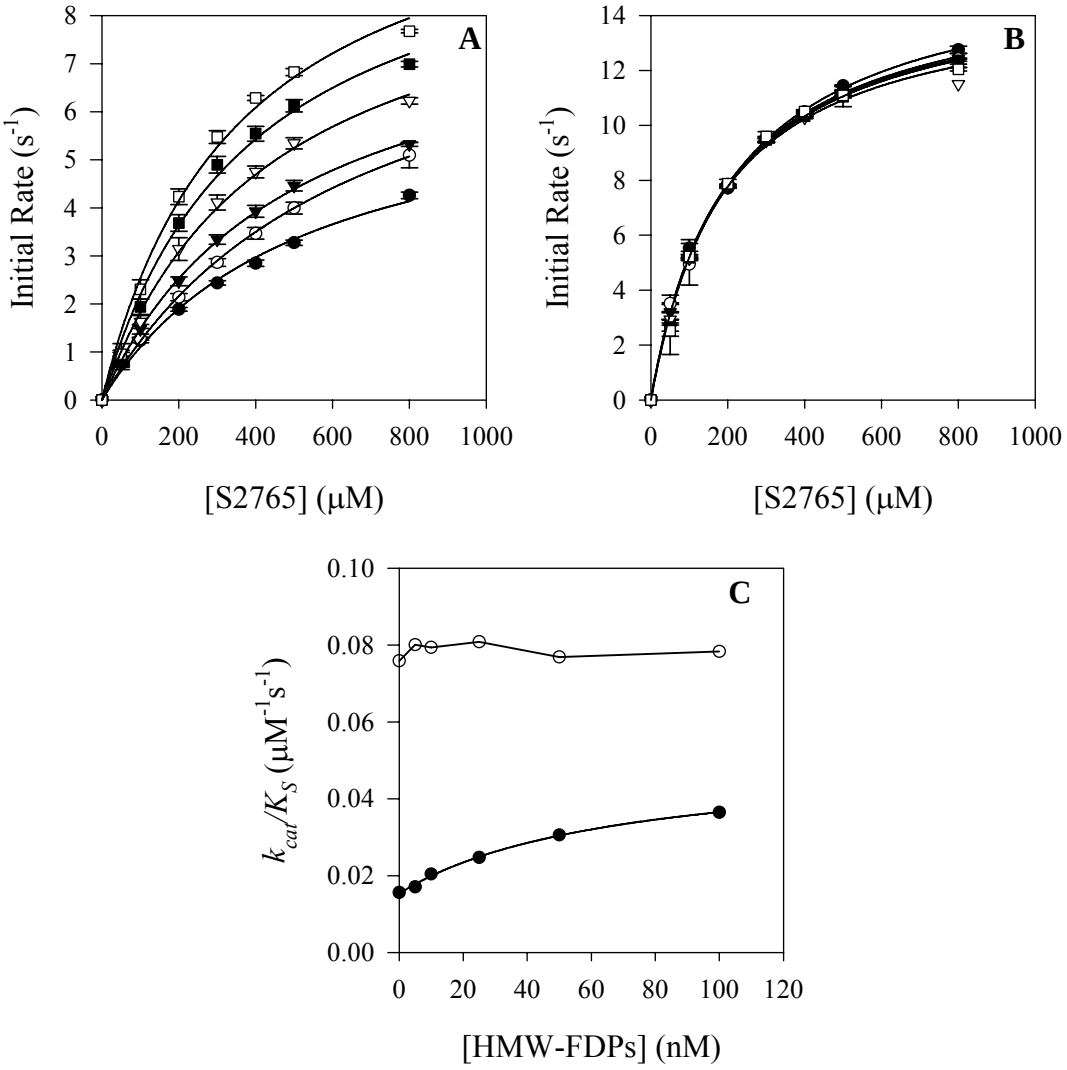

Figure 3-8. k_{cat}/K_S Values Vary with HMW-FDP Concentration for tPA but not tc-tPA. The k_{cat} and K_S values were determined from the initial rate of S2765 hydrolysis by tPA (*A*) and tc-tPA (*B*) as described. The k_{cat}/K_S values (*C*) for tPA (*closed circles*), but not tc-tPA (*open circles*), were fit to a 3 parameter hyperbolic function.

of HMW-FDPs, k_2 showed little change from 0-500 nM Vn (Fig. 3-9). In the presence of 100 nM HMW-FDPs, a modest decrease in k_2 from 0.69×10^6 $M^{-1}s^{-1}$ to 0.47×10^6 $M^{-1}s^{-1}$ was observed. This observation is consistent with previously published data indicating that Vn does not alter the rate at which PAI-1 inhibits tPA (75).

HMW-FDPs Protect tPA from Inhibition by PAI-1 – Previous studies have shown that fibrin protects tPA from inhibition by PAI-1 (76,77). The raw absorbance data in Fig. 3-10A shows that as the HMW-FDP concentration increases, the absorbance at the endpoint also increases. In other words, tPA activity is maintained for a longer period of time in the presence of HMW-FDPs. Thus, the HMW-FDPs are protecting tPA from inhibition by PAI-1. HMW-FDPs decreased k_2 3.4-fold from 2.75×10^6 $M^{-1}s^{-1}$ to 0.80×10^6 $M^{-1}s^{-1}$ at 100 nM HMW-FDPs and 3.9-fold at saturation (0.71×10^6 $M^{-1}s^{-1}$) with tPA (Fig. 3-10*B*). When tc-tPA was the activator, k_2 decreased from 6.57×10^6 $M^{-1}s^{-1}$ to 2.47×10^6 $M^{-1}s^{-1}$ at 100 nM HMW-FDPs and 0.80×10^6 $M^{-1}s^{-1}$ at saturation, a 2.7-fold and 8.2-fold decrease respectively (Fig. 3-10*C*). The k_2 values for tPA and tc-tPA inhibition by PAI-1 in the absence of HMW-FDPs are consistent with previously measured values (37,38,78,79). As hypothesized, PAI-1 inhibits tc-tPA twice as fast as tPA in the absence of HMW-FDPs. This observation is consistent with others that have also shown that PAI-1 inhibits tc-tPA faster than sc-tPA (36-38).

TAFIa Does Not Change the HMW-FDP Dependent Protection of tPA from PAI-1 – tPA is able to bind fibrin through its finger and kringle 2 domains. To investigate if TAFIa alters protection, the HMW-FDPs were treated with TAFIa to remove the carboxyl-terminal lysine and arginine residues. Similar to the untreated HMW-FDPs, TAFIa treated HMW-FDPs protected tPA from PAI-1 inhibition 4.5-fold at 100 nM (Fig.

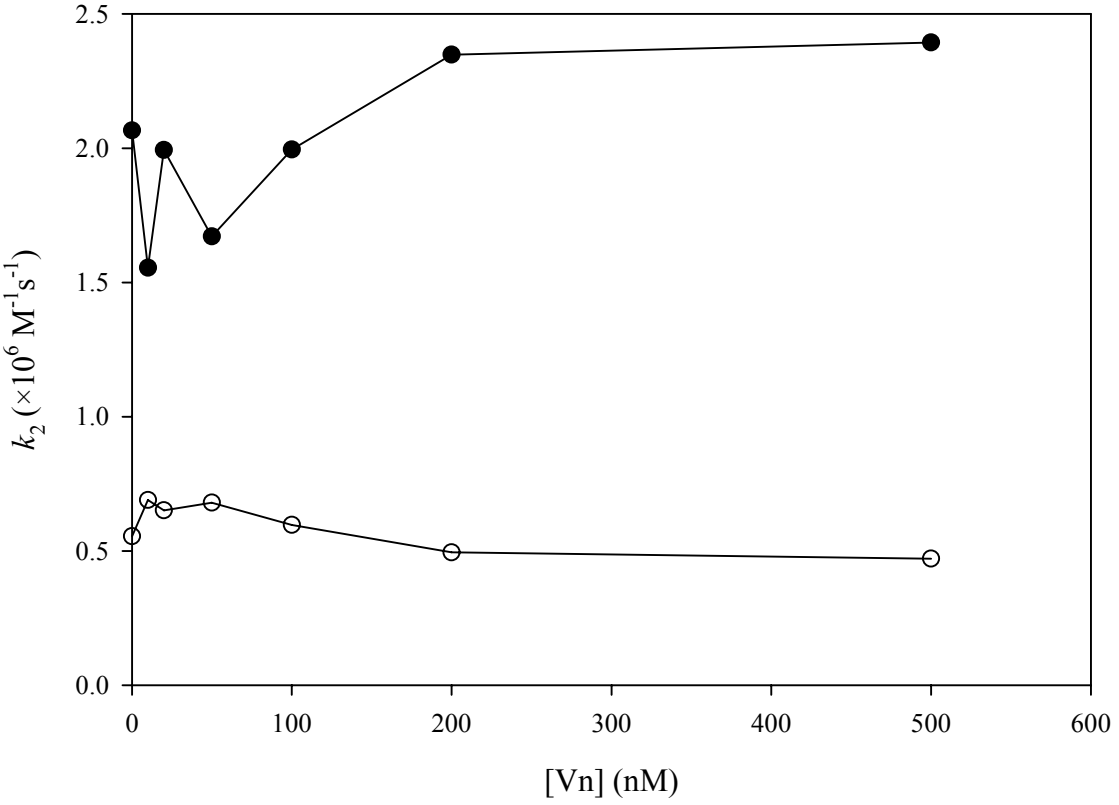

Figure 3-9. Vn Does not Appreciably Alter the Rate of tPA Inhibition by PAI-1. Endpoint assays were performed with Vn in the presence of tPA (5 nM), PAI-1 (10 nM), and S2765 (400 μM) at 0 nM (*closed circles*) and 100 nM (*open circles*) HMW-FDPs. k_2 was calculated from each end point as described.

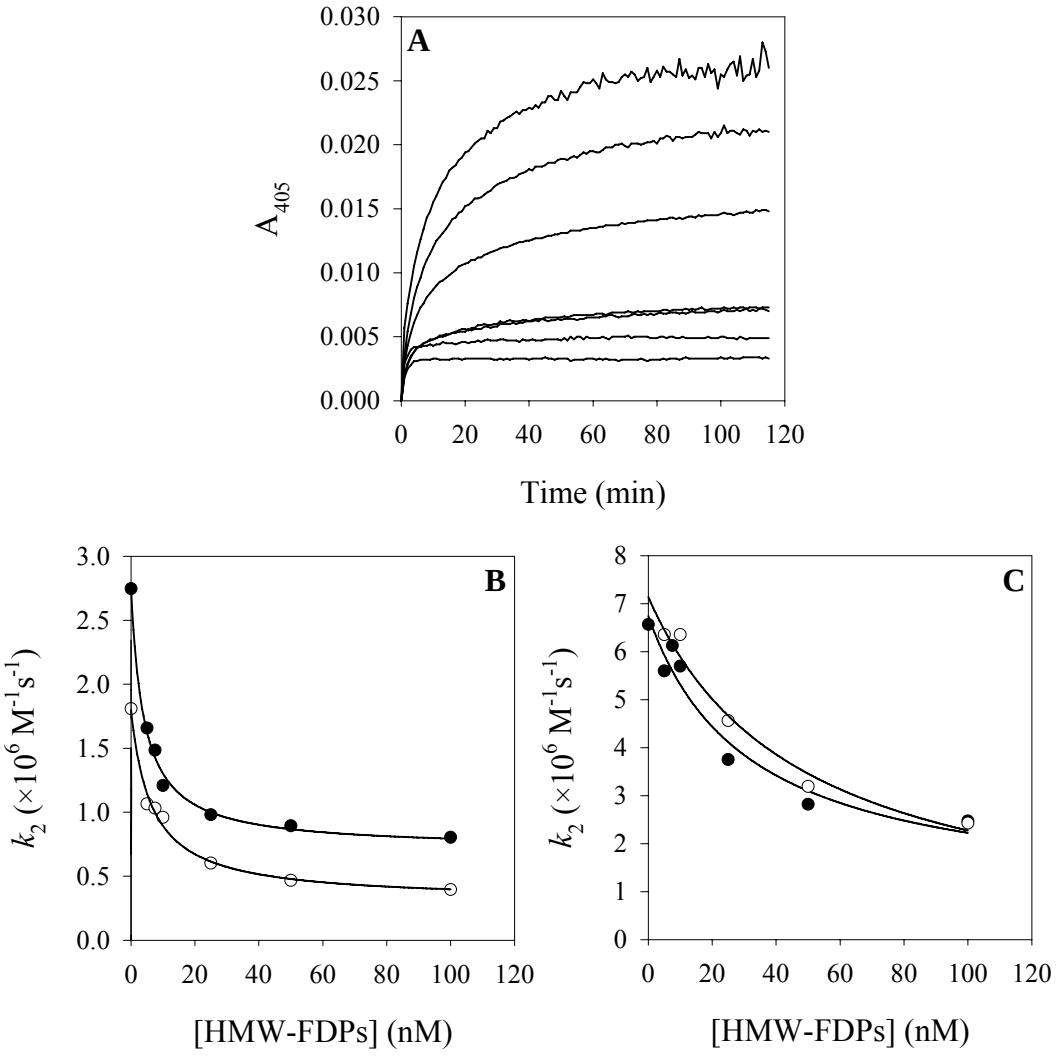

Figure 3-10. HMW-FDP treatment with TAFIa does not alter their ability to protect tPA from inhibition by PAI-1. Both unmodified HMW-FDPs (*closed circles*) and TAFIa treated HMW-FDPs (*open circles*) in the presence of PAI-1 (10 nM), Vn (200 nM), and S2765 (400 μM) were added to either tPA (*B*) or tc-tPA (*C*). k_2 was calculated from each end point as described. The change in absorbance due to S2765 hydrolysis is shown in panel A for the reaction performed with tPA. From bottom to top, the HMW-FDP concentrations range from 0-100 nM.

3-10*B*); k_2 decreased by 2.9-fold at 100 nM TAFIa treated HMW-FDPs with tc-tPA as the activator (Fig. 3-10*C*).

5IAF-Pg Further Protects tPA from PAI-1 Inhibition – Because Pg is also able to bind fibrin through its kringle domains, it is conceivable that Pg plays some role in retarding the rate of tPA inhibition. By using 5IAF-Pg as a substrate instead of S2765, end point assays revealed that 5IAF-Pg reduced the inhibition rate of tPA by PAI-1. 5IAF-Pg decreased k_2 by 3.6-, 4.9-, 8.5-, and 8.7-fold at 25, 50, 75, and 100 nM HMW-FDPs respectively in the presence of tPA (Fig. 3-11*A*). Using tc-tPA, 5IAF-Pg decreased k_2 6.5-, 10.9-, 9.4-, and 8.2-fold over the same HMW-FDP concentrations (Fig. 3-11*B*).

The HMW-FDPs were treated with TAFIa to remove the carboxyl-terminal lysine and arginine residues, and thus Pg binding. TAFIa treated HMW-FDPs protected tPA from inhibition by 3.3-fold (Fig. 3-12). In other words, TAFIa treatment eliminated virtually all the protection afforded by 5IAF-Pg; the remaining protection is provided by the HMW-FDPs alone.

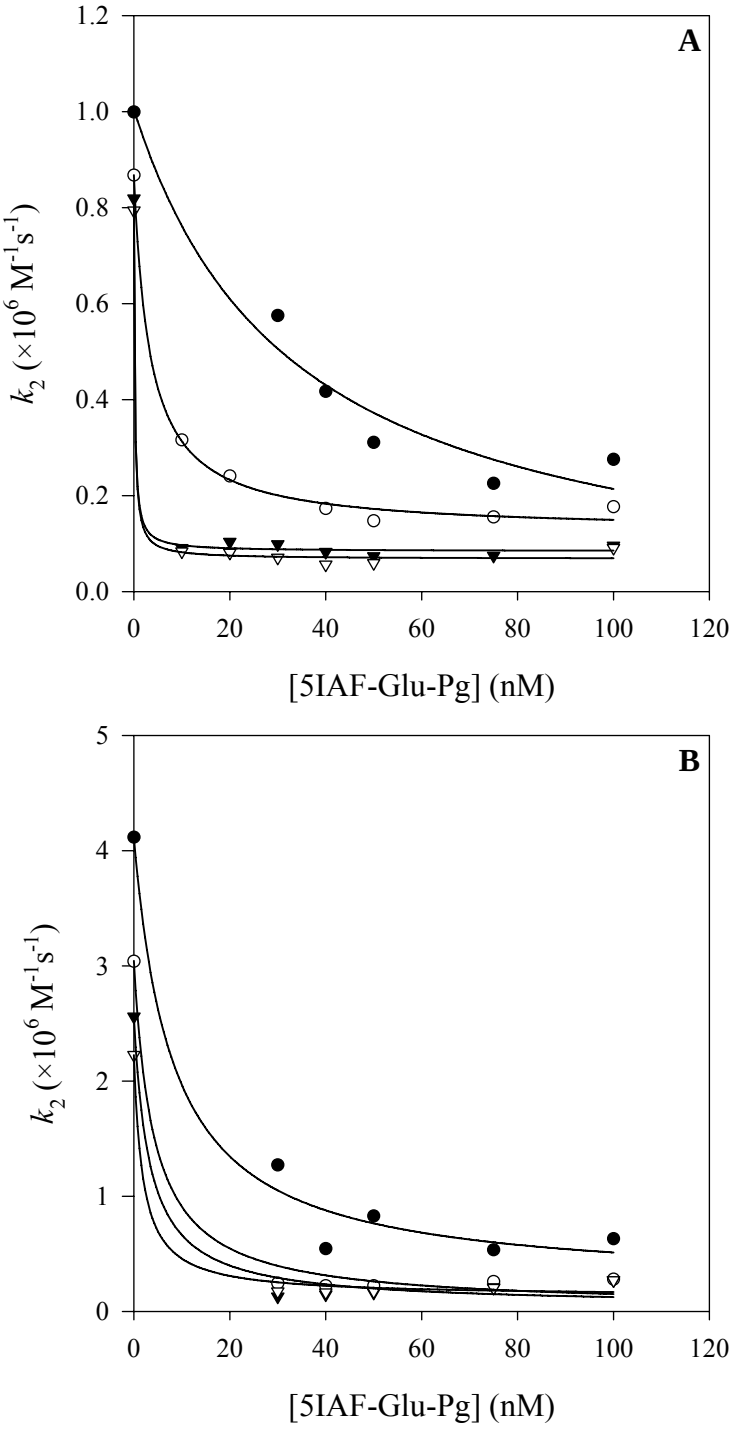

Figure 3-11. tPA protection from PAI-1 by 5IAF-Pg in the presence of HMW-FDPs. HMW-FDPs at 25 nM (*closed circles*), 50 nM (*open circles*), 75 nM (*closed triangles*), and 100 nM (*open triangles*) each with Vn (200 nM) and 5IAF-Pg were added to 5 nM tPA (*A*) or tc-tPA (*B*). The PAI-1 concentration was 15 nM for assays at 75 and 100 nM HMW-FDPs with tPA; otherwise, experiments were performed with 10nM PAI-1. k_2 was calculated from the end points as described.

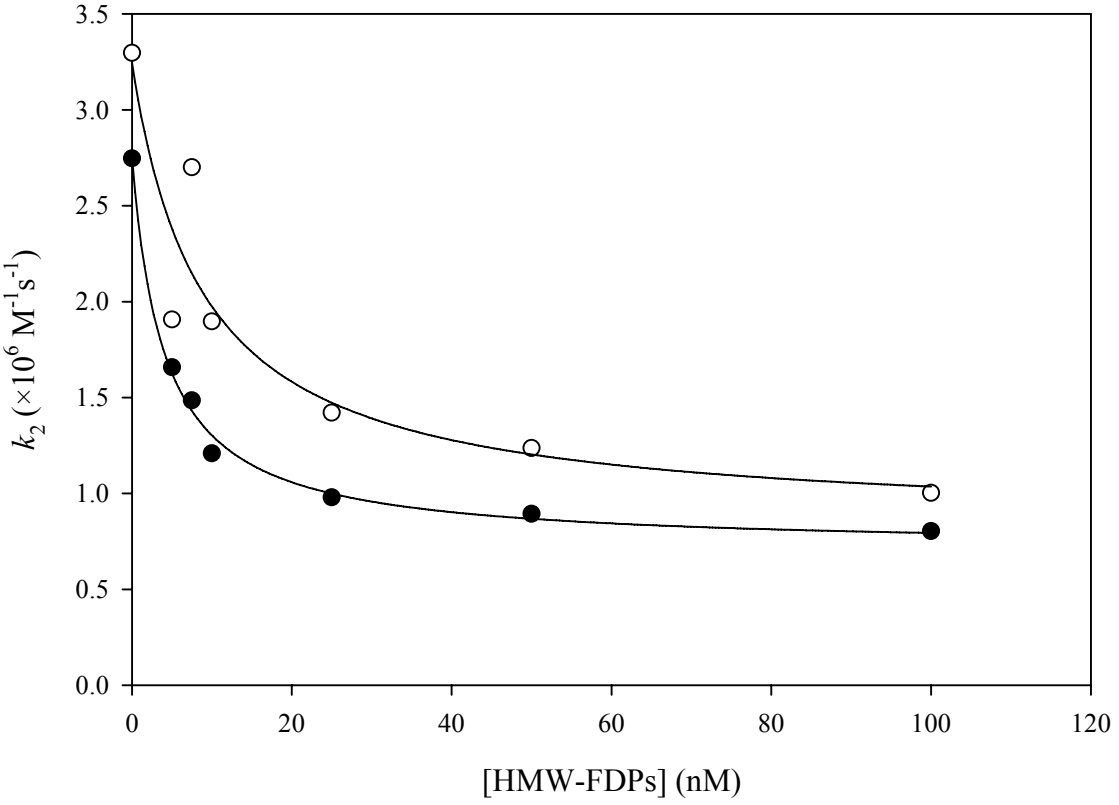

Figure 3-12. TAFIa treatment of the HMW-FDPs removes the protection provided by 5IAF-Pg. Unmodified HMW-FDPs (*closed circles*) and TAFIa treated HMW-FDPs containing 100 nM 5IAF-Pg (*open circles*) were added to tPA (5 nM) in the presence of PAI-1 (10 nM), Vn (200 nM), and S2765 (400μM). Using the end points, k_2 was calculated as described.

4. Discussion

Glu- and Lys-Pg Activation on Fibrin. HMW-FDPs and intact fibrin were used to study the effects of TAFIa on Lys-Pg activation and Lys-Pn inhibition by AP respectively. TAFIa treatment dramatically decreased the cofactor activity of HMW-FDPs for both Glu- and Lys-Pg activation. The k_{cat}/K_m for 5IAF-Glu-Pg cleavage on intact fibrin, HMW-FDPs, and TAFIa treated HMW-FDPs were 0.142 (31), 10.6, and 0.0254 $\mu M^{-1}s^{-1}$, and 2.69 (31), 192, and 3.50 $\mu M^{-1}s^{-1}$ for 5IAF-Lys-Pg cleavage. TAFIa treated HMW-FDPs are a 5.6-fold less effective cofactor than intact fibrin for 5IAF-Glu-Pg cleavage, but an equally good cofactor for 5IAF-Lys-Pg cleavage. Based on the catalytic efficiencies, TAFIa suppresses Glu-Pg activation 7.6 times more than Lys-Pg. In other words, Lys-Pg, while a 19-fold better substrate on fibrin and an 18-fold better substrate on Pn modified fibrin, is a 138-fold better substrate than Glu-Pg on TAFIa modified fibrin. Much of the difference between Glu- and Lys-Pg activation is likely due to the difference in the affinity of both Glu- and Lys-Pg for the HMW-FDPs after TAFIa treatment. Furthermore, the K_m increased upon TAFIa treatment, which resulted in a depressed activation rate. However, both changes are less dramatic for Lys-Pg than Glu-Pg. As a result, considerable Lys-Pg activation occurs even on TAFIa treated HMW-FDPs.

Because TAFIa treated HMW-FDPs are a much better cofactor for Lys-Pg activation than Glu-Pg activation, it raises the possibility of two separate sites for Pg binding on HMW-FDPs, and in turn fibrin. Previous experiments by Nesheim *et al.* (33) showed that fibrin binds Lys-Pg but not Glu-Pg. The first site is certainly one of the carboxyl-terminal lysines exposed by Pn. The second site for Lys-Pg, however, remains uncertain,

although an internal lysine remains the most likely candidate, as Pg mediates binding through its kringle domains. Presumably, Lys-Pg can bind both sites with similar affinities, but Glu-Pg only weakly interacts with the second site. 5IAF-Glu-Pg binding to TAFIa treated HMW-FDPs displayed an increase in fluorescence (Fig. 3-1C); all other binding between 5IAF-Pg and HMW-FDPs decreased in fluorescence. One explanation is that this increase is monitoring the weak interaction of Glu-Pg to the second site on HMW-FDPs.

Glu- and Lys-Pn Protection from AP by Fibrin. Based on the observations of Bajzar *et al.* (52), TAFIa surprisingly prolonged clot lysis in the presence of Lys-Pg. Bajzar *et al.* (52), who added TAFI to their clot lysis experiments, saw no prolongation with Lys-Pg. Because Lys-Pg is a 19-fold better substrate on fibrin than Glu-Pg, enough Pn to lyse the clot was likely generated before enough TAFIa accumulated to prolong lysis. In the present experiments, TAFIa was added. The decrease in the cofactor activity of fibrin depressing Lys-Pg activation was enough to prolong lysis, despite no TAFIa mediated attenuation of Lys-Pn inhibition by AP. If thrombomodulin had been included in the experiments of Bajzar *et al.* (52), they would likely have seen prolongation as TAFI activation would have occurred at a much faster rate.

TAFIa removes much of the protection associated with Pn modified fibrin, primarily due to the suppression of free Pn within the clot (Fig. 3-5). However, when Lys-Pg is used in place of Glu-Pg, there is only a modest decrease (1.8-fold versus 6-fold) in protection as well as free Pn (Fig. 3-6). Thus, Lys-Pn is protected 16-fold better in the presence of TAFIa than Glu-Pn. One reaction that was not quantified in this system was the Glu- to Lys-Pg/Pn conversion. Presumably, the Pn made in the presence of TAFIa is

Glu-Pn. When TAFIa decays to the point where it can no longer effectively eliminate the exposed carboxyl-terminal lysines, Pn reaches some steady-state level sufficient to convert Glu-Pg and Glu-Pn to their Lys forms. Lastly, the Pn peak that appears just before lysis is likely almost all Lys-Pn. In other words, the Pn that ultimately degrades the clot into FDPs is Lys-Pn.

Fig. 4-1 summarizes the relationship between lysis, k_2, and $[Pn]_f$. In the absence of TAFIa (Fig. 4-1A), k_2 decreased to 1.8×10^6 $M^{-1}s^{-1}$ shortly after clotting and at the same time, $[Pn]_f$ began to slowly increase. Once Pn modifies fibrin, displayed by a decrease in turbidity, $[Pn]_f$ rose to a steady state and k_2 concurrently decreased, highlighting the increased protection associated with Pn modified fibrin. During the plateau in $[Pn]_f$, Pn likely began generating Lys-Pg/Pn, which results in a sharp increase in $[Pn]_f$, due to positive feedback, and subsequently clot lysis. Once the clot dissolved, Pn protection from AP decreased causing $[Pn]_f$ to subside. In Fig. 4-1B, TAFIa noticeably prolongs the generation of Pn modified fibrin, which results in a low $[Pn]_f$ and increased k_2. Once the TAFIa decayed, Pn modified fibrin was generated, k_2 decreased, and $[Pn]_f$ rapidly increased, eventually lysing the clot. When Glu-Pg is replaced with Lys-Pg (Figs. 4-1C and D), the Pn modified fibrin was made shortly after clotting in both the presence and absence of TAFIa. Lys-Pn was equally protected in both cases as noticed by little change in k_2. Thus, the decreased $[Pn]_f$, caused by a decreased Lys-Pg activation rate, is the major reason for the increase in the clot lysis time in the presence of TAFIa.

The Glu-to Lys-Pg/Pn conversion potentially serves as a switch to lyse the clot. In plasma, TAFI activation occurs immediately following clot formation (unpublished observations by J.H. Foley and M.E. Nesheim). TAFIa shuts down lysis by suppressing

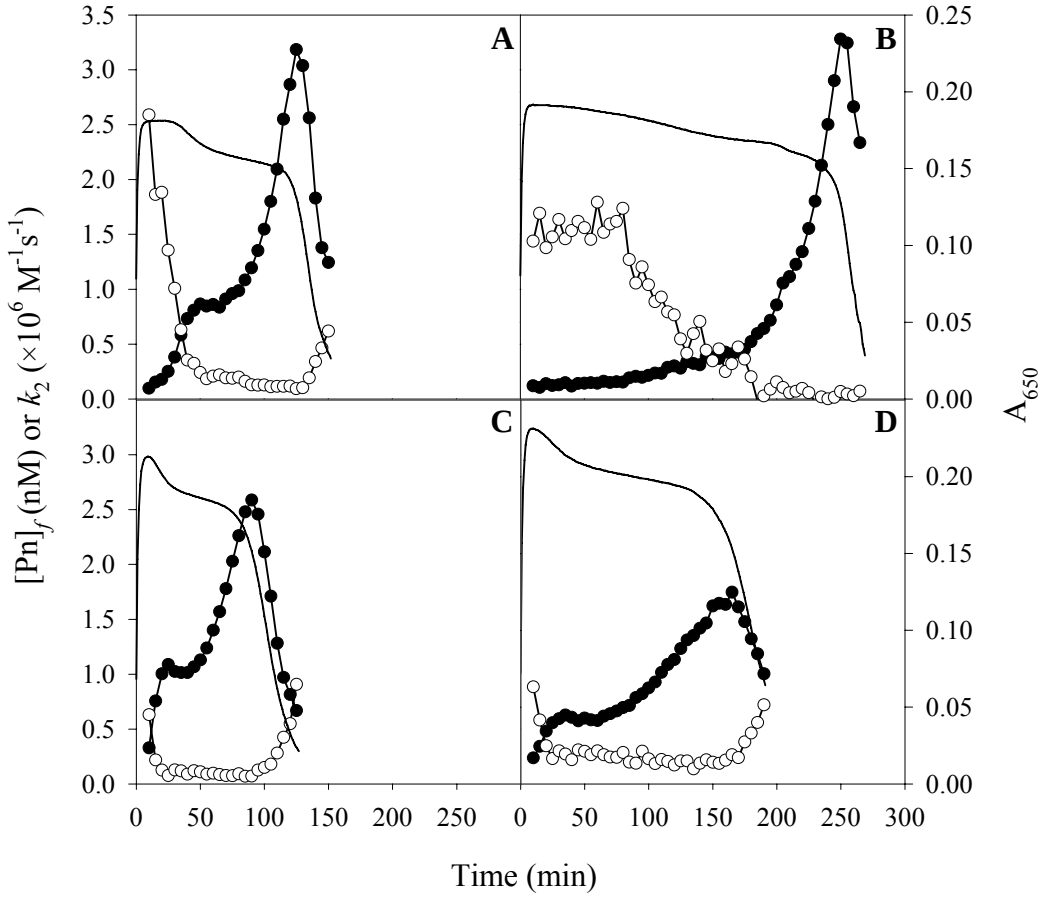

Figure 4-1. A summary of the effects of TAFIa on clot lysis. The clot lysis profile (solid line), $[Pn]_f$ (*closed circles*), and k_2 (*open circles*) over time are shown for the clots formed in the presence of Glu-Pg with no TAFIa (*A*) and with 500 pM TAFIa (*B*) and Lys-Pg with no TAFIa (*C*) and with 500 pM TAFIa (*D*).

Glu-Pg activation, Glu- to Lys-Pg conversion, and increasing the rate of Glu-Pn inhibition. Upon TAFIa decay, Pn levels rise, reaching a steady state, due to an increased activation rate and a decrease in the inhibition rate. The Glu- to Lys- conversion begins generating the positive feedback for Pn generation by increasing its rate of formation. Once Lys-Pn forms, the clot lyses. The question that remains, however, is what potential function or role does Lys-Pn have considering Glu- and Lys-Pn are equally protected in the absence of TAFIa? Others have shown that Pn is capable of activating TAFI (53). If TAFIa were generated at any point during lysis in the presence of Glu-Pn, lysis would likely cease because it would be rapidly inhibited. In the presence of Lys-Pn, any TAFIa generated would have little to no effect on inhibition and therefore lysis. Thus, Lys-Pn generation serves as a point where lysis occurs with no known mechanism available to stop its progress.

tPA Protection from PAI-1 by Fibrin and Pg. Fibrin acts as a cofactor for its own degradation by providing a binding surface for the major fibrinolytic proteins, namely tPA and Pg. Multiple mechanisms exist to regulate the breakdown of the fibrin clot. Before the clot starts releasing degradation products, Pn modifies the fibrin surface, exposing carboxyl-terminal lysine and arginine residues. The exposure of the lysine residues up regulates Pg activation and increases the lifetime of Pn by decreasing its susceptibility to inhibition by AP (47). While Pn modification generates a protective surface for Pn, the same can be said for tPA. HMW-FDPs protected tPA from PAI-1 inhibition by 3-5 fold (Fig. 3-10). When the HMW-FDPs were treated with TAFIa, no alteration in protection was seen. Because tPA binds fibrin through a finger domain (lysine independent) and a kringle 2 domain (lysine dependent), the observed protection

is likely mediated by the finger domain. TAFIa is not able to eliminate tPA binding; thus, TAFIa modified HMW-FDPs are still able to protect tPA.

Previous work has shown that TAFIa removes the exposed carboxyl-terminal lysine and arginine residues and as a result prolongs clot lysis (46). This modification removes the positive feedback loop for Pn formation as well as increases the rate of Pn inhibition by AP (47,65). As demonstrated in this study, HMW-FDPs and 5IAF-Pg together were able to protect tPA by 24-30 fold. TAFIa modification of the HMW-FDPs eliminated the additional 8-10 fold protection provided by 5IAF-Pg, highlighting a novel mechanism whereby TAFIa can modulate tPA levels. Without carboxyl-terminal lysine residues, Pg is no longer able to bind the HMW-FDPs and therefore no longer compete with PAI-1 for the active site of tPA.

For the first time, the effect of Pg on the rate of tPA inhibition has been quantified. A recurrent problem when working with fibrin surfaces and other fibrin surrogates is their degradation by Pn. In this study, a recombinant Pg mutant, in which the active site serine has been mutated to a cysteine and labeled with 5IAF, was used in place of native Pg. This Pg derivative does not generate active Pn that can feedback and cleave the HMW-FDPs, exposing additional carboxyl terminal lysine and arginine residues, thereby nullifying the TAFIa modification.

In the absence of HMW-FDPs, PAI-1 inhibits tc-tPA 2-3 times faster than tPA, a result corroborated by others (36-38). This result illustrates a potential negative feedback mechanism for Pn generation. Previous work determined that low levels of Pn are still generated within a clot containing TAFIa (47). While this steady-state level is not sufficient to lyse the clot, it may be able to cleave tPA into its two chain form, thereby

increasing its vulnerability to inhibition by PAI-1. Thus, Pn action on sc-tPA would down regulate fibrinolysis in the presence of PAI-1. Pn levels in the presence of TAFIa are suppressed by not only eliminating Pg binding, but by slowing its activation. TAFIa has the ability to modulate both Pn and tPA levels, and therefore fibrinolysis, by altering the capability of Pn modified fibrin to protect tPA from inhibition by PAI-1.

Previous work has reported that Vn binds PAI-1 with a nanomolar affinity (80). Because the plasma Vn concentration is over 100 fold greater than the plasma PAI-1 concentration, PAI-1 likely circulates in complex with Vn. As reported here (Fig. 3-9) and by others (75), Vn does not affect the rate of tPA inhibition by PAI-1. However, Vn does stabilize the PAI-1, increasing its half life by 2-3 fold (81). Evidently, the role of Vn is not to alter inhibition kinetics, but to stabilize PAI-1 and to localize it to fibrin (74,82).

Although the effect of TAFIa modification of fibrin on the rate of tPA inhibition has been investigated, the question of how the various forms of fibrin change the inhibition rate over the course of clotting and subsequent lysis still remains. Because tPA does not involve the typical zymogen to serine protease cleavage, such a question would be difficult to measure because there is no constant supply of tPA. One would expect that intact fibrin would protect tPA similar to TAFIa modified fibrin because both forms still contain the finger binding site. In the absence of fibrin, tPA is rapidly inhibited. Upon clotting, intact fibrin would reduce the inhibition rate 3-5 fold, sufficient to generate low levels of Pn. Shortly after clotting, TAFI activation occurs to rapidly remove any carboxyl-terminal lysine residues exposed by the actions of Pn, thus suppressing lysis. After TAFIa decays due to its thermal instability, new carboxyl-terminal lysines are

generated by Pn cleavage of fibrin to which Pg can bind, causing a 24-30 fold reduction in the rate of tPA inhibition. The result is increased Pg activation and subsequent lysis. Following lysis, tPA would be rapidly inhibited again, thus shutting off the fibrinolytic cascade.

Future Directions – The results and conclusions presented in this thesis suggest further lines of investigation that could be pursued. In one of these, experiments could be designed to chronically activate TAFI over long periods of time (hours) to sustain a fixed TAFIa concentration and thereby determine whether TAFIa absolutely inhibits fibrinolysis. In another, the lysis times could be measured at various doses of Lys-Pg, but keeping the total Pg concentration constant to determine if the Lys-Pg pathway could circumvent the TAFIa mediated prolongation of lysis. In yet another, experiments could be performed to probe the hypothesis proposed in this work that Pn cleavage of tPA promotes the down regulation of fibrinolysis.

References

1. Redman, C. M. and Xia, H. (2000) *Fibrinolysis Proteolysis* **14,** 198-205

2. Erickson, H. P. and Fowler, W. E. (1983) *Ann.N.Y.Acad.Sci.* **408,** 146-163

3. Everse, S. J., Pelletier, H., and Doolittle, R. F. (1995) *Protein Sci.* **4,** 1013-1016

4. Doolittle, R. F., Spraggon, G., and Everse, S. J. (1998) *Curr.Opin.Struct.Biol.* **8,** 792-798

5. Yang, Z., Kollman, J. M., Pandi, L., and Doolittle, R. F. (2001) *Biochemistry* **40,** 12515-12523

6. Doolittle, R. F. (2003) *J.Thromb.Haemost.* **1,** 1559-1565

7. Weisel, J. W., Veklich, Y., and Gorkun, O. (1993) *J.Mol.Biol.* **232,** 285-297

8. Lorand, L., Credo, R. B., and Janus, T. J. (1981) *Methods Enzymol.* **80,** 333-342

9. Weisel, J. W., Francis, C. W., Nagaswami, C., and Marder, V. J. (1993) *J.Biol.Chem.* **268,** 26618-26624

10. Mosesson, M. W., Siebenlist, K. R., Hainfeld, J. F., and Wall, J. S. (1995) *J.Structural Biol.* **115,** 88-101

11. Nesheim, M. (2003) *Chest* **124,** 33S-39S

12. Walker, J. B. and Nesheim, M. E. (1999) *J.Biol.Chem.* **274,** 5201-5212

13. Esmon, C. T., Esmon, N. L., and Harris, K. W. (1982) *J.Biol.Chem.* **257,** 7944-7947

14. Esmon, N. L., Carroll, R. C., and Esmon, C. T. (1983) *J.Biol.Chem.* **258,** 12238-12242

15. Esmon, N. L. (1989) *Prog.Hemost.Thromb.* **9,** 29-55

16. Weiler, H. and Isermann, B. H. (2003) *J.Thromb.Haemost.* **1,** 1515-1524

17. Nagashima, M., Lundh, E., Leonard, J. C., Morser, J., and Parkinson, J. F. (1993) *J.Biol.Chem.* **268,** 2888-2892

18. Wang, W., Nagashima, M., Schneider, M., Morser, J., and Nesheim, M. (2000) *J.Biol.Chem.* **275,** 22942-22947

19. Kisiel, W., Canfield, W. M., Ericsson, L. H., and Davie, E. W. (1977) *Biochemistry* **16,** 5824-5831

20. Walker, F. J., Sexton, P. W., and Esmon, C. T. (1979) *Biochim.Biophys.Acta* **571,** 333-342

21. Walker, F. J., Chavin, S. I., and Fay, P. J. (1987) *Arch.Biochem.Biophys.* **252,** 322-328

22. Sottrup-Jensen, L., Claeys, H., Zajdel, M., Petersen, T. E., and Magnusson, S. (1978) *Prog.Chem.Fibrinolysis Thrombolysis* **3,** 191-209

23. Markus, G., De Pasquale, J. L., and Wissler, F. C. (1978) *J.Biol.Chem.* **253,** 727-732

24. Lerch, P. G., Rickli, E. E., Lergier, W., and Gillessen, D. (1980) *Eur.J.Biochem.* **107,** 7-13

25. Hochschwender, S. M. and Laursen, R. A. (1981) *J.Biol.Chem.* **256,** 11172-11176

26. Thorsen, S., Clemmensen, I., Sottrup-Jensen, L., and Magnusson, S. (1981) *Biochim.Biophys.Acta* **668,** 377-387

27. Novokhatny, V. V., Matsuka, Y., and Kudinov, S. A. (1989) *Thromb.Res.* **53,** 243-252

28. Menhart, N., Sehl, L., Kelley, R. F., and Castellino, F. J. (1991) *Biochemistry* **30,** 1948-1957

29. McCance, S. G., Menhart, N., and Castellino, F. J. (1994) *J.Biol.Chem.* **269,** 32405-32410

30. Marti, D., Schaller, J., Ochensberger, B., and Rickli, E. E. (1994) *Eur.J.Biochem.* **219,** 455-462

31. Horrevoets, A. J. G., Pannekoek, H., and Nesheim, M. E. (1997) *J.Biol.Chem.* **272,** 2183-2191

32. Pannekoek, H., de Vries, C., and van Zonneveld, A. J. (1988) *Fibrinolysis* **2,** 123-132

33. Nesheim, M., Fredenburgh, J. C., and Larsen, G. R. (1990) *J.Biol.Chem.* **265,** 21541-21548

34. Levin, E. G., Marzec, U., Anderson, J., and Harker, L. A. (1984) *J.Clin.Invest* **74,** 1988-1995

35. Rijken, D. C., Hoylaerts, M., and Collen, D. (1982) *J.Biol.Chem.* **257,** 2920-2925

36. Chmielewska, J., Ranby, M., and Wiman, B. (1988) *Biochem.J.* **251,** 327-332

37. Thorsen, S., Philips, M., Selmer, J., Lecander, I., and Astedt, B. (1988) *Eur.J.Biochem.* **175,** 33-39

38. Lawrence, D. A., Strandberg, L., Ericson, J., and Ny, T. (1990) *J.Biol.Chem.* **265,** 20293-20301

39. Walker, J. B. and Nesheim, M. E. (2001) *J.Biol.Chem.* **276,** 3138-3148

40. Takada, A., Watahiki, Y., and Takada, Y. (1986) *Thromb.Res.* **41,** 819-827

41. Fredenburgh, J. C. and Nesheim, M. E. (1992) *J.Biol.Chem.* **267,** 26150-26156

42. Wang, W., Hendriks, D. F., and Scharpe, S. S. (1994) *J.Biol.Chem.* **269,** 15937-15944

43. Tan, A. K. and Eaton, D. L. (1995) *Biochemistry* **34,** 5811-5816

44. Campbell, W. and Okada, H. (1989) *Biochem.Biophys.Res.Commun.* **162,** 933-939

45. Bajzar, L., Morser, J., and Nesheim, M. (1996) *J.Biol.Chem.* **271,** 16603-16608

46. Wang, W., Boffa, M. B., Bajzar, L., Walker, J. B., and Nesheim, M. E. (1998) *J.Biol.Chem.* **273,** 27176-27181

47. Schneider, M. and Nesheim, M. (2004) *J.Biol.Chem.* **279,** 13333-13339

48. Fuentes-Prior, P., Iwanaga, Y., Huber, R., Pagila, R., Rumennik, G., Seto, M., Morser, J., Light, D. R., and Bode, W. (2000) *Nature* **404,** 518-525

49. Le Bonniec, B. F., MacGillivray, R. T. A., and Esmon, C. T. (1991) *J.Biol.Chem.* **266,** 13796-13803

50. Le Bonniec, B. F. and Esmon, C. T. (1991) *Proc.Natl.Acad.Sci.USA* **88,** 7371-7375

51. Schneider, M., Nagashima, M., Knappe, S., Zhao, L., Morser, J., and Nesheim, M. (2002) *J.Biol.Chem.* **277,** 9944-9951

52. Bajzar, L., Manuel, R., and Nesheim, M. E. (1995) *J.Biol.Chem.* **270,** 14477-14484

53. Mao, S. S., Cooper, C. M., Wood, T., Shafer, J. A., and Gardell, S. J. (1999) *J.Biol.Chem.* **274,** 35046-35052

54. Leurs, J., Wissing, B. M., Nerme, V., Schatteman, K., Bjorquist, P., and Hendriks, D. (2003) *Thromb.Haemost.* **89,** 264-271

55. Zhao, L., Morser, J., Bajzar, L., Nesheim, M., and Nagashima, M. (1998) *Thromb.Haemost.* **80,** 949-955

56. Brouwers, G. J., Vos, H. L., Leebeek, F. W. G., Bulk, S., Schneider, M., Boffa, M., Koschinsky, M., van Tilburg, N. H., Nesheim, M. E., Bertina, R. M., and García, E. B. G. (2001) *Blood* **98,** 1992-1993

57. Schneider, M., Boffa, M., Stewart, R., Rahman, M., Koschinsky, M., and Nesheim, M. (2002) *J.Biol.Chem.* **277,** 1021-1030

58. Boffa, M. B., Bell, R., Stevens, W. K., and Nesheim, M. E. (2000) *J.Biol.Chem.* **275,** 12868-12878

59. Schneider, M. and Nesheim, M. (2003) *J.Thromb.Haemost.* **1,** 147-154

60. Walker, J. B., Hughes, B., James, I., Haddock, P., Kluft, C., and Bajzar, L. (2003) *J.Biol.Chem.* **278,** 8913-8921

61. Giles, A. R., Tinlin, S., and Greenwood, R. (1982) *Blood* **60,** 727-730

62. Broze, G. J. Jr. and Higuchi, D. A. (1996) *Blood* **88,** 3815-3823

63. Mosnier, L. O., Lisman, T., Van den Berg, H. M., Nieuwenhuis, H. K., Meijers, J. C. M., and Bouma, B. N. (2001) *Thromb.Haemost.* **86,** 1035-1039

64. Walker, J. B. and Bajzar, L. (2004) *J.Biol.Chem.* **279,** 27896-27904

65. Schneider, M., Brufatto, N., Neill, E., and Nesheim, M. (2004) *J.Biol.Chem.* **279,** 13340-13345

66. van Zonneveld, A. J., Veerman, H., and Pannekoek, H. (1986) *J.Biol.Chem.* **261,** 14214-14218

67. de Vries, C., Veerman, H., and Pannekoek, H. (1989) *J.Biol.Chem.* **264,** 12604-12610

68. Horrevoets, A. J. G., Smilde, A., de Vries, C., and Pannekoek, H. (1994) *J.Biol.Chem.* **269,** 12639-12644

69. Brufatto, N. and Nesheim, M. E. (2001) *J.Biol.Chem.* **276,** 17663-17671

70. Boffa, M. B., Wang, W., Bajzar, L., and Nesheim, M. E. (1998) *J.Biol.Chem.* **273,** 2127-2135

71. Horrevoets, A. J. G., Pannekoek, H., and Nesheim, M. E. (1997) *J.Biol.Chem.* **272,** 2176-2182

72. Bajzar, L., Fredenburgh, J. C., and Nesheim, M. E. (1990) *J.Biol.Chem.* **265,** 16948-16954

73. Neill, E. K., Stewart, R. J., Schneider, M. M., and Nesheim, M. E. (2004) *Anal.Biochem.* **330,** 332-341

74. Podor, T. J., Peterson, C. B., Lawrence, D. A., Stefansson, S., Shaughnessy, S. G., Foulon, D. M., Butcher, M., and Weitz, J. I. (2000) *J.Biol.Chem.* **275,** 19788-19794

75. Keijer, J., Ehrlich, H. J., Linders, M., Preissner, K. T., and Pannekoek, H. (1991) *J.Biol.Chem.* **266,** 10700-10707

76. Kruithof, E. K. O., Tran-Thang, C., Ransijn, A., and Bachmann, F. (1984) *Blood* **64,** 907-913

77. Masson, C. and Angles-Cano, E. (1988) *Biochem.J.* **256,** 237-244

78. Madison, E. L., Goldsmith, E. J., Gerard, R. D., Gething, M. J. H., Sambrook, J. F., and Bassel-Duby, R. S. (1990) *Proc.Natl.Acad.Sci.USA* **87,** 3530-3533

79. Shubeita, H. E., Cottey, T. L., Franke, A. E., and Gerard, R. D. (1990) *J.Biol.Chem.* **265,** 18379-18385

80. Salonen, E. M., Vaheri, A., Pollanen, J., Stephens, R., Andreasen, P., Mayer, M., Dano, K., Gailit, J., and Ruoslahti, E. (1989) *J.Biol.Chem.* **264,** 6339-6343

81. Declerck, P. J., Mol, M. D., Alessi, M. C., Baudner, S., Paques, E. P., Preissner, K. T., Muller-Berghaus, G., and Collen, D. (1988) *J.Biol.Chem.* **263,** 15454-15461

82. Podor, T. J., Campbell, S., Chindemi, P., Foulon, D. M., Farrell, D. H., Walton, P. D., Weitz, J. I., and Peterson, C. B. (2002) *J.Biol.Chem.* **277,** 7520-7528